

**Versican Expression During Embryonic Development in the Mouse**

**Jessica M. Snyder**

**A thesis**

**submitted in partial fulfillment of the  
requirements for the degree of**

**Master of Science**

**University of Washington**

**2014**

**Committee:**

**Charles Frevert**

**Mary Chang**

**Thea Brabb**

**Ida Washington**

**Program Authorized to Offer Degree:**

**Comparative Medicine**

©Copyright 2014

Jessica M. Snyder

University of Washington

**Abstract**

Versican Expression During Embryonic Development in the Mouse

Jessica M. Snyder

Chair of the Supervisory Committee:

Charles Frevert, DVM ScD

Department of Comparative Medicine

Versican is a chondroitin sulfate proteoglycan and a component of the extracellular matrix that has previously been shown to have an important role during the embryonic development of many organs. In this study, versican expression in the head, heart, lung and liver was tracked during development in the mouse. Versican gene expression and quantitative  $\beta$ -GAG immunohistochemistry performed from embryonic day (E) 11.5 to E15.5 showed peak versican expression at E13.5 in the lung and the brain. Quantitative  $\beta$ -GAG immunohistochemistry and mRNA analysis of the embryonic head, liver, and lung had identical patterns of versican expression. Versican degradation, as measured by DPEAAE immunoreactivity, showed an inverse pattern of expression compared to  $\beta$ -GAG immunoreactivity, and there was co-localization of  $\beta$ -GAG and DPEAAE positive staining, suggesting complementary roles of versican deposition and degradation in embryogenesis.

## **Dedication**

This thesis is dedicated to my loving (and patient) family: Dave, Jacob, and Ava, and to my parents, for all of their encouragement and support.

## **Acknowledgements**

I would like to acknowledge Erin McCarty for assistance embedding embryos and preparing unstained slides and Cara Appel for assistance with quantitative immunohistochemistry.

## Table of Contents

Introduction.....	1
Materials and Methods.....	6
Results.....	12
Discussion.....	20
Liver.....	20
Heart.....	21
Brain.....	22
Lung.....	24
Conclusions.....	28
Figures.....	29
References.....	49

## Introduction

Versican, a member of the lectican family, is the largest chondroitin sulfate proteoglycan and a component of the extracellular matrix which has an important role in the development of the lung, heart, musculoskeletal system, and central nervous system [1],[2],[3],[4],[5],[6],[7]. The structure of versican is characterized by an approximately 550 kDa core protein consisting of an amino-terminal (G1) domain which binds hyaluronan and a carboxy-terminal (G3) domain, as well as two central chondroitin sulfate glycosaminoglycan attachment domains, the GAG  $\alpha$  and GAG  $\beta$  domains [5],[8],[9],[10] (Figure 1). Versican has 4 different isoforms: V0 (which contains both  $\alpha$  and  $\beta$  GAG chains), V1 (which contains only the  $\beta$  chain), V2 (which contains only the  $\alpha$  chain), and V3 (which contains neither GAG chain) [8],[11] (Figure 1). V1 versican promotes cell growth, aggregation, and a mesenchymal-epithelial transition, while the V2 isoform appears to have an inhibitory effect [11],[12],[13],[14]. The V2 (most likely exclusive to brain), V3, V1, and V0 isoforms are present in adult tissues [8],[10],[15]. The V0 and V1 isoforms predominate during embryonic development and decrease rapidly at birth [3],[7],[10],[16],[17]. In one study, expression of V0 and V1 decreased in brain by 90% after birth to a baseline, low adult level [7]. Through interactions with hyaluronan and other extracellular matrix molecules and cell surface proteins, versican plays an important role in regulating cell behaviors such as cell adhesion, migration, proliferation, differentiation, apoptosis, morphogenesis, and extracellular matrix and water content maintenance [5],[6],[12],[18],[19],[20],[21],[22].

Versican is present at low levels in most adult tissues and is increased with inflammation [23]. V2 versican is normally present in the adult central nervous system, predominantly in

white matter, in some neuronal somata and dendrites, and potentially in the perineuronal net extracellular matrix [10],[11],[24]. Versican in the CNS inhibits neural differentiation and neurite growth and is increased following injury and altered in pathological conditions such as multiple sclerosis [11],[14],[25],[26],[27]. In the lung, versican accumulation is increased in such pathological conditions as acute respiratory distress syndrome (ARDS), chronic obstructive pulmonary disease (COPD), sarcoidosis, tuberculosis, extrinsic allergic alveolitis, and experimentally induced asthma [22],[23],[28],[29],[30].

In a previous study, the highest level of versican expression in the mouse was detected at embryonic day (E) 13.5, with a 21 day gestation typical for the mouse, and the versican signal detected in the whole embryonic mouse was much higher than in adult tissues [31]. In adults, the highest expression of versican is found in the brain, with the least expression in the liver and intermediate expression in the lung and heart [31]. In the developing brain, the roles of the V0 and V1 isoforms in neural differentiation, neural crest cell migration, and neurite outgrowth have been studied [16],[32],[33]. Immunohistochemistry performed in chick embryos showed absence of versican in migration pathways and presence of versican expression in barrier tissues, which suggests an important function of versican in formation of the peripheral nervous system by guiding neural crest cells and axons to target regions [16]. Embryonic neural crest stem cells from the mouse have also been shown to avoid V0/V1 containing substrates in vitro [34]. Both V0/V1 and V2 gene expression have been demonstrated in neuronal precursor cells and glial lineage cells isolated from E16 rat spinal cord and in cerebral cortex from E16 and E19 rats and P0 and P7 mice [10],[11],[35]. Increasing levels of the V2 isoform by  $\alpha$ -GAG immunohistochemistry have been reported in the developing rodent brain after P18 [7],[36].

Changes in versican gene expression and immunohistochemistry during development have been well characterized in the heart [5],[37]. Versican is critical in cardiac atrioventricular canal (AVC) cushion development and ventricular septal formation, and versican deficient mice develop fatal cardiac defects by E10.5 [4],[5]. Studies performed in later term murine embryos have shown a significantly higher versican expression in embryonic as compared to adult aorta [38].

In the lung, previous work in the mouse suggests peak versican gene expression at E13.5, with a subsequent notable decline over time to E18.5 [39]. Immunohistochemical studies performed in the mouse have also shown versican distribution throughout the lung at E16.5, with immunostaining present in the lung mesenchyme and around the basement membrane of the bronchiolar epithelium [40]. Studies in sheep have shown distribution of versican throughout the perialveolar region at all embryonic ages evaluated, with a decrease in versican lung expression in the perisaccular and alveolar regions over the last trimester of pregnancy associated with a reduction in lung tissue volume [3]. These results suggest an important role of versican in structural lung development [3].

Versican immunohistochemistry is performed using an  $\alpha$ -GAG or a  $\beta$ -GAG antibody, which react with the V2 and V1 versican isoforms, respectively [7],[10],[35] (Figure 1). Previous studies in embryonic mice have shown stronger  $\beta$ -GAG than  $\alpha$ -GAG staining in tissues of the developing murine limb and human fetal spine, consistent with predominance of the V1 isoform during embryonic development [41],[42]. Previous work has shown both  $\alpha$ -GAG and  $\beta$ -GAG reactivity in the developing rodent brain, although the distribution of immunostaining

differs somewhat for the two antibodies as areas such as the fimbria of the hippocampus and Purkinje cells are positive only on  $\alpha$ -GAG versican immunohistochemistry in late gestation [35].

Versican and other proteoglycans are degraded by a family of A Disintegrin and Metalloproteinase with ThromboSpondin motifs (ADAMTS) proteinases [43],[44],[45]. Cleavage of V1 versican by ADAMTS-1, -4, -5, and -9 results in an approximately 70 kilodalton fragment containing the neoepitope sequence DPEAAE [17],[43],[45],[46],[47],[48],[49]. Previous studies have shown increased DPEAAE immunoreactivity adjacent to areas of versican immunoreactivity in the embryonic mouse limb and heart [46],[50],[51]. Versican and ADAMTS expression have also been shown to overlap and co-localize in the embryonic heart and lung suggesting increased proteolysis of versican during development [40],[50]. ADAMTS-1 reactivity was the most pronounced in one study of embryonic limb development in the mouse [46], and ADAMTS-1 also has been shown to be strongly expressed in the rodent embryonic brain, heart, lung, limb, liver, spleen and kidney [50],[52],[53]. The highest expression of ADAMTS-1 in one study of embryonic mice occurred in the kidney, pancreas, lung, heart, and placenta in late gestation (E16) [53]. In a study using embryonic rats, ADAMTS-1 expression decreased in later embryonic ages and in adult tissues [52]. ADAMTS-4 appears to be sparsely expressed during mouse embryonic development [46],[50]. ADAMTS-5 is expressed in many tissues during mouse development (brain, limb muscle, tendon, and interdigital mesenchyme) [40]. Severe developmental abnormalities have not been noted in either *Adamts-1* or *Adamts-5* knockout mice, although *Adamts-1*<sup>-/-</sup> mice are smaller than wild type mice with reduced fertility and renal changes and a mild increase in cardiac valve size in late embryonic development in *Adamts-5*<sup>-/-</sup> mice has been reported [54],[55]. It is possible that there is redundancy or

compensation for the loss of one ADAMTS proteinase by the others in terms of versican proteolysis [40],[56]. Developmental anomalies such as syndactyly and cleft palate have been described in murine models with compound ADAMTS gene mutations [43],[57],[58].

The goal of this project was to track changes in versican expression via polymerase chain reaction and immunohistochemistry in the brain, heart, liver, and lung during embryonic development at five time points in the mouse. The hypothesis was that total versican expression would change with key developmental events but would generally tend to decrease with increasing gestational age. A secondary goal of this project was to track versican degradation products during embryonic development, with a particular focus on the developing nervous system and lung, with the hypothesis that DPEAAE versican fragments would inversely correlate with total versican expression. A five day time frame during development centered on E13.5 was chosen, as this day has previously been shown to have the highest versican expression in the total mouse embryo and in the developing mouse lung. Changes in versican gene expression and quantitative versican and DPEAAE immunohistochemistry over this time period in the embryonic mouse lung and brain have not previously been reported.

## **Materials and Methods**

### *Animal Model*

C57Bl6/J wild type mice (The Jackson Laboratory, Bar Harbor, ME) housed under standard conditions and a 12:12 dark: light cycle were time mated approximately 1 hour prior to the onset of the dark cycle and were checked for presence of a vaginal plug the following morning. Embryos were considered to be gestational age 0.5 days (E0.5) on the morning that the vaginal plug was identified. E11.5-E15.5 (inclusive) embryos were harvested in the morning. Embryos were staged to ensure age appropriate development, and embryos that did not appear developmentally age appropriate were excluded [59]. Three litters for each time point were collected, with a median of 7 embryos per litter and 20 embryos per time point collected. Embryos were harvested and placed in ice-cold phosphate buffered saline (PBS) solution. From each litter harvested, three randomly-selected embryos were used for immunohistochemistry and the remaining embryos were used for mRNA isolation. Cerebrum, heart, liver, and lung samples were harvested from six 8-12 week old male and female C57Bl6/J mice and used as controls. All procedures were performed as part of an approved scientific protocol in accordance with the University of Washington Institutional Animal Care and Use Committee (IACUC).

### *Quantitative Real Time Reverse Transcription-PCR*

Embryos used for mRNA isolation were dissected and the head, whole heart, whole lung, and whole liver were removed and placed in RNAlater (AMBION, Austin, Texas) at a 1:10 ratio and stored at 4°C for less than 1 week until processing. Head, heart, lung, and liver from all of the embryos in the litter were pooled by organ for mRNA isolation, with the exception of heads

from E13.5 and older embryos, which were processed separately due to their larger size. For E13.5 and later embryos, the face and snout was dissected from the head and removed prior to processing. Tissues from six adult mice were collected immediately following CO<sub>2</sub> euthanasia and included a section of cerebral cortex, sagittal section of heart incorporating atria, valve, and ventricle, portion of liver lobe excluding gall bladder, and section of peripheral lung excluding trachea and primary bronchi. Tissues for immunohistochemistry (brain, removed in its entirety and sectioned in the sagittal plane; liver; lung; and heart) were harvested from three of these adult wild type C57Bl/6 mice following CO<sub>2</sub> euthanasia.

For mRNA isolation, tissues were removed from RNAlater and placed in 1:100 lysis buffer with beta-mercaptoethanol. Tissues were homogenized for 20-40 seconds and centrifuged for 4 minutes at 400xG. RNA was extracted from the supernatant using RNeasy Mini Kit as directed by the manufacturer (QIAGEN, [www.qiagen.com](http://www.qiagen.com)) and cDNA was reverse transcribed using random primers with the High Capacity cDNA Reverse Transcription Kit as directed by the manufacturer (Applied Biosystems, Foster City, CA). Quantitative real time reverse transcription polymerase chain reaction (PCR) was performed on a ABI Prism 7900HT Fast Real-Time PCR System using Taq Man Universal PCR Master Mix Reagents as directed by the manufacturer (Applied Biosystems, Foster City, CA). The ABI Gene Expression Assays used are as follows: versican, Hs00171642\_m1;18S, Hs99999901\_s1; V0 primer (MUV0), A1X00D8; V1 primer, Mm00490173\_m1; V2 primer (MUV2), A1WR170; V3 primer, Rn01493763\_m1; ADAMTS1, Mm00477355\_m1. The ABI Gene Expression Assay forward and reverse primers are proprietary. Normalized mRNA levels were then expressed as -fold of levels in adult control tissues using the comparative cycle threshold (*Ct*) method. Delta *Ct* ( $\Delta C_t$ )

was calculated as the difference in  $Ct$  values for the target genes compared to 18S and relative mRNA was calculated as  $2^{-\Delta\Delta Ct}$  as previously described [60],[61].

Total versican PCR was performed two times per sample for the liver and heart and three times per sample for the lung and head. Versican isoform PCR (V0 primer, V1 primer, V2 primer, V3 primer) was performed once for the lung and head, with all samples on a single plate. PCR was performed once with all of the samples on a single plate with the Versican V3 plasmid (mouse) total versican standard (generous gift of Kathleen Braun, Benaroya Research Institute) at dilutions of  $3 \times 10^5$  copies,  $3 \times 10^4$  copies,  $3 \times 10^3$  copies,  $3 \times 10^2$  copies, 30 copies, and 0 copies/9  $\mu$ L. A versican standard curve was constructed relating  $Ct$  value to versican copy number. The copy number for the embryonic tissues based on versican mRNA  $Ct$  values for 15ng cDNA was calculated according to this standard curve using the equation: Copy number =  $e^{(-0.7482 * Ct + 29.4752)}$ .

#### *Versican and DPEAAE Quantitative Immunohistochemistry*

Embryos for immunohistochemistry (IHC) were removed from the embryonic membranes, fixed in 10% neutral buffered formalin for approximately 24-48 hours, and then transferred to 70% ethanol for approximately 24-72 hours prior to processing. Embryos at 14.5 and 15.5 days post conception were chilled on ice until anesthetized and immobile and were either decapitated or transected caudal to the thorax with sharp scissors prior to formalin fixation. Embryos were routinely paraffin embedded with three embryos per litter on one slide positioned in the same orientation and sectioned along the sagittal plane to include brain, heart, lung, and

liver. Heart, lung, liver, and brain from 8-12 week old adult control mice harvested following euthanasia by carbon dioxide asphyxiation were routinely processed and paraffin embedded.

The primary antibody to detect versican accumulation was the  $\beta$ -GAG antibody (Millipore #1033, lot #2006928) for one hour at 2  $\mu$ g/mL following pretreatment with Chondroitinase ABC for 1 hour and HIER1 (Citrate) for 10 minutes. Immunohistochemistry for the  $\alpha$ -GAG antibody (Millipore #1032) at 2  $\mu$ g/ml for one hour following pretreatment with Chondroitinase ABC for 1 hour and HIER1 (Citrate) for 10 minutes was also performed on one litter (three individual embryos) of E12.5 embryos and two litters (three embryos per litter) of E13.5 embryos. Immunohistochemistry was performed for DPEAAE-reactive versican fragments using the  $\alpha$ DPE Vc neopeptide (Thermoscientific #PA1-1748A, lot#NE161982) at 2.5  $\mu$ g/mL (Primary antibody) for 1 hour with HIER2 (EDTA) for 10 minutes.

Slides were scanned in Brightfield at a 20X objective using a Nanozoomer Digital Pathology slide scanner (Hamamatsu; Bridgewater, New Jersey). The digital images were then imported into Visiopharm software (Hoersholm, Denmark) for analysis. Using the Visiopharm Image Analysis module, regions of interest (ROIs) were manually drawn around relevant areas. The software was then trained to label Versican-positive or DPEAAE-positive staining versus unstained tissue using a project-specific configuration based on a threshold of pixel values. The images were processed in batch using this configuration to generate the desired outputs (area of Versican, ratio of Versican to total tissue area, area of DPEAAE, and ratio of DPEAAE to total tissue area).

A sample image of organ measurements obtained is provided (Figure 2). Head and brain measurements were obtained separately. Brain was measured exclusive of the ventricle. Head was measured exclusive of the snout and soft tissue to approximate the sample obtained for mRNA analysis. If the organ was not visible or substantially damaged during processing, then analysis was not performed. Based on output for each embryo analyzed, the mean value for each organ at each embryonic age was calculated by averaging the results for the three embryos in each litter and then averaging the three litters from each embryonic age.

### *Statistics*

Statistics and images were generated in GraphPad Prism (San Diego, California). For PCR analyses of total versican gene expression, the fold increase over the adult control was calculated for each embryo litter on two separate runs for liver and heart and three separate runs for head and lung. Three litters per time point were used for E11.5, E12.5, and E15.5. Four litters per time point were used for E13.5 and E14.5. Values from each PCR run for fold increase over adult control of each embryo litter were averaged and the result was log transformed to yield an approximately normal distribution. For PCR analyses of the four versican isoforms, the fold increase over adult control was calculated for each embryo litter on one run for the lung and head samples only. For  $\beta$ -GAG versican and DPEAAE quantitative immunohistochemistry analyses, the ratio of positive staining to total tissue area was calculated for each organ in each embryo and values from mice in the same litter were averaged and log transformed to yield an approximately normal distribution. Age and organ comparisons for PCR and quantitative immunohistochemistry data were analyzed by one way ANOVA followed by

Tukey's post test. Statistical results with a p-value  $< 0.05$  were considered statistically significant.

## Results

*Versican relative mRNA is highest in the lung and head at E13.5, and by E15.5 an adult pattern of relative versican expression is present, with the highest expression in the brain and lowest expression in the liver.*

All of the embryonic tissues had higher levels of versican gene expression by PCR than the adult controls (Figure 3). The embryonic head had significantly higher versican gene expression than the adult brain at E13.5, E14.5, and E15.5 ( $p < 0.05$ ). The embryonic heart had significantly higher versican gene expression than the adult heart at E12.5 and E13.5 ( $p < 0.05$ ). The embryonic liver had significantly higher versican gene expression than the adult liver at E11.5, E12.5, and E13.5 ( $p < 0.05$ ). The embryonic lung had significantly higher versican gene expression than the adult lung at E11.5, E12.5, E13.5, and E14.5 ( $p < 0.05$ ). In the adult, the liver had the least versican expression (27 copy numbers per 15ng cDNA) and the brain had the most versican expression (1705 copy numbers per 15ng cDNA). Versican gene expression in the heart and lung was intermediate, with 1435 copy numbers and 552 copy numbers per 15ng cDNA, respectively.

Among the embryonic tissues, the liver had the least versican gene expression at every time studied (Figure 3). Further, versican gene expression in the liver varied significantly by time ( $p = 0.0024$ ) and versican expression decreased significantly from E11.5 to E15.5 ( $p < 0.05$ ). Versican expression in the liver by *Ct* value for 15ng cDNA was significantly lower than in the lung and heart at E11.5 and than in the lung, heart and head at E12.5, E13.5, E14.5, and E15.5 ( $p < 0.05$ ). Versican gene expression in the head increased from E11.5 to E15.5, and at E15.5 the

head had the highest versican gene expression (lowest *Ct* value, highest copy number) of all of the organs. Versican gene expression in the head was significantly higher at E13.5 than at E11.5 and E12.5 ( $p < 0.05$ ). Versican gene expression in the lung was greatest at E13.5, although this difference was not statistically significant. At E11.5, the heart had the highest versican gene expression of the organs tested, and the versican expression was lower at E15.5 than at E11.5, although this difference also was not statistically significant. At E15.5, the pattern of relative versican gene expression for the organs tested was the same as in the adult, with the highest expression in the brain, lowest expression in the liver, and intermediate expression in the heart and lung (Figure 3). The highest cumulative versican gene expression in the head, heart, liver, and lung occurred at E13.5 (Figure 3).

***The relative gene expression of the versican isoforms V0 and V1 is high in embryonic lung and head, and the relative gene expression of the V2 isoform increases with time in the embryonic head but not in the lung.***

Gene expression of the four versican isoforms was evaluated over time in the lung and the brain (Figure 4). Relative mRNA expression (fold increase over adult control) was highest for V0 and V1 at all time points both in the head and the lung. In the head, V0 and V1 isoform gene expression was significantly higher at E13.5 than at E11.5 and E12.5 ( $p < 0.05$ ), and the V0 isoform expression in embryonic head was also significantly higher at E15.5 than E11.5 ( $p < 0.05$ ). In the lung, V0 and V1 isoform expression did not vary significantly over time. Gene expression of the V2 isoform in lung was similar to that of the adult control tissue at every embryonic time point and did not vary significantly at any embryonic age (normalized *Ct* value for adult control = 23.1 for 15ng cDNA; *Ct* value for E11.5 to E15.5 lung = 23.9 to 24.4 for 15ng

cDNA) (Figure 5). However, the normalized *Ct* value for the V2 isoform in the brain of the adult control and in the embryonic heads varied significantly (normalized adult *Ct* value = 19.5 for 15ng cDNA; E11.5 *Ct* value = 22.8; E12.5 *Ct* value = 21.7; E13.5 to E15.5 *Ct* values = 20.1 to 20.13 for 15ng cDNA;  $p=0.0004$ ), and the relative V2 isoform expression in the head was significantly higher at E13.5, E14.5, and E15.5 than at E11.5 ( $p<0.05$ ) and significantly higher at E13.5 than at E12.5 ( $p<0.05$ ) (Figure 5). While the relative V3 mRNA expression was similar for embryonic and adult lung samples tested (V3 isoform expression in embryonic lung ranged from 0.7 to 1.3 times that of adult control lung tissue), the relative V3 mRNA expression for embryonic head ranged from 4.2 (E11.5) to 10.6 (E13.5) times that of the adult control brain tissue. Relative gene expression of the V3 isoform did not vary significantly by embryonic age in the lung but was significantly higher at E13.5 than at E12.5 in the head ( $p<0.05$ ).

***ADAMTS1 gene expression is similar in the adult and embryonic head, heart, and liver, but not in the lung.***

In contrast to versican, the relative gene expression of ADAMTS1 for the embryonic organs was similar to that of the adult control tissue for the head, heart, and liver. In the embryonic head, relative ADAMTS-1 gene expression ranged from 1.3 to 4 times that in the adult brain. In the embryonic heart, relative ADAMTS-1 gene expression ranged from 1.5 to 2.1 times that of the adult control at the time points tested. In the embryonic liver, relative ADAMTS-1 gene expression ranged from 0.6 to 1.5 times that of the adult control at the various time points. ADAMTS1 relative mRNA expression in the adult lung was higher than in the other organs, and therefore the relative mRNA expression in the embryonic lung was

approximately 10% that of the adult lung at most time points tested. There was no significant difference in ADAMTS-1 gene expression with embryonic age in any of the organs studied.

***Quantitative  $\beta$ -GAG versican immunohistochemistry mirrors versican mRNA expression.***

Representative images from embryos at E11.5, E12.5, E13.5, E14.5, and E15.5 are shown (Figures 6-10).  $\beta$ -GAG versican immunostaining throughout most of the organs of the embryo was seen, although consistently little positivity was seen in the liver. In the lung at all ages there was strong immunoreactivity to the  $\beta$ -GAG antibody. At E11.5 to E12.5, there was strong staining of the mesenchyme of the lung bud (the scaffolding for lung development), with little positive staining in airway (Figures 6 and 7). At E13.5, very strong staining was present through the mesenchyme including the periphery of the lung and the basement membrane, with little to no immunopositivity of the developing epithelium (Figures 8 and 11). At E14.5 and E15.5, there was marked expansion of airways and alveolar space with little immunoreactivity of the epithelial cells, strong positivity of the basement membrane, and moderate to strong immunoreactivity of the mesenchyme, although areas of reduced immunoreactivity in the regions surrounding the bronchi and along the outer surfaces of lung were noted compared to earlier gestational ages (Figures 9, 10, and 11). There was significantly greater  $\beta$ -GAG versican immunoreactivity of the lung at E13.5 compared to E11.5 ( $p < 0.05$ ).

In the brain at E11.5, there was a single ventricle with weak  $\beta$ -GAG immunopositivity of a surrounding thin rim of cortex and relatively little white matter. The strongest staining at this age was present in the deep cortex and the developing white matter, as well as in the roof of the fourth ventricle. Pronounced staining of the mesenchyme of the developing skull, nasal process, and jaw was present (Figure 6). At E12.5, there was increased immunoreactivity noted in the

roof of the neopallial cortex and midbrain and in the deep layers of the developing medulla and pons/midbrain. Increased and more clearly defined white matter was present at this stage, with immunoreactivity especially of the white matter just deep to the developing gray matter, such as the corpus striatum (Figure 7). At E13.5 the choroid plexus was just apparent and little immunopositivity in the cells of the choroid plexus was noted, but staining in the connective tissue stalk supporting the choroid was noted. There was increased white matter at this stage, and positive staining of the white matter was appreciated. Also at this stage, there was an increasingly laminar appearance to the cortex with increased immunoreactivity of the roof of the neopallial cortex and roof of the midbrain and immunopositivity of the developing olfactory lobe. There was very strong, homogeneous staining of the upper lip, palatal shelf of the maxilla, and primordial cartilage at this stage. There was little staining of the ganglion of the fifth cranial nerve and the semicircular canals and ganglion of the eighth cranial nerve (Figure 8). At E14.5 and E15.5, increasing convolution and organization of the neural tube and ventricular system was apparent. There was less staining in cortical gray matter and no staining was noted in the epithelial cells of the choroid plexus. The white matter was expanded and strongly stained, although slightly less intensely compared to E13.5, at E14.5 and E15.5. There was strong staining of the cerebellar primordium at E14.5 and E15.5 (Figures 9 and 10). There was significantly greater versican immunoreactivity of the brain at all ages compared to the adult control ( $p < 0.05$ ).

The liver had the least  $\beta$ -GAG versican staining by quantitative immunohistochemistry at all of the time points tested, and the amount of positive staining decreased significantly over time (Figure 12). The liver had the most pronounced  $\beta$ -GAG versican immunoreactivity at

E11.5, with mild to moderate intracellular (nuclear) and lesser extracellular staining. At E12.5, there was a notable decrease in the number of positive cells, with some positivity in the cytoplasm. In later stages, there was virtually no positive staining in the liver, with only mild staining of occasional blood vessels. There was significantly greater  $\beta$ -GAG versican staining in the liver at E11.5 compared to E14.5, E15.5, and the adult control ( $p < 0.05$ ). The liver had significantly less  $\beta$ -GAG immunoreactivity than the lung and the brain at all embryonic times tested ( $p < 0.05$ ).

The brain and the head had identical patterns of  $\beta$ -GAG versican staining over time, with the head consistently higher than the brain (Figure 13). The pattern of  $\beta$ -GAG versican immunoreactivity over time in the brain and the head mirrored the mRNA results, with a lower value at E11.5 and E12.5 and then increased values at the older time points, with the highest value at E13.5 (Figures 13 and 14).

Very little positive  $\beta$ -GAG versican staining was noted in the adult brain (1.8% ratio of positive versican expression to total tissue area); liver (0.4% positive expression); lung (0.05% positive expression); and heart (0.4% positive expression).

***Quantitative DPEAAE immunohistochemistry inversely correlates with  $\beta$ -GAG immunoreactivity.***

The liver also had the least positive staining by quantitative immunohistochemistry for DPEAAE at all of the time points tested, and the amount of positive staining did not vary significantly over time. Weak cytoplasmic immunoreactivity was noted at E11.5; at subsequent stages, virtually no immunoreactivity was noted, and so few positive regions were seen both on

DPEAAE and versican immunohistochemistry that it was difficult to co-localize areas of positive staining. The liver had significantly less DPEAAE staining than the brain and lung at E14.5 and E15.5 ( $p < 0.05$ ).

The pattern of DPEAAE immunoreactivity was the inverse of the pattern of  $\beta$ -GAG versican immunoreactivity for the lung and the brain; when the versican immunoreactivity was greatest, the DPEAAE was lower, and vice versa (Figure 15). For the brain, anti-DPEAAE positive staining decreased significantly from E11.5 to E13.5 ( $p < 0.05$ ). The DPEAAE immunoreactivity was significantly higher at every embryonic time tested than in the adult control ( $p < 0.05$ ). In the developing brain, there was weak overall staining at E11.5 and E12.5, and staining was most pronounced in the cortex. At E13.5, there was increased positivity of the cortex and in cortical cells lining the ventricle. There was mild intranuclear staining of cells in the deeper layers of the gray matter and mild immunopositivity in the developing white matter, which increased in the white matter and developing medulla at E14.5. At E15.5, there was increased staining in the white matter and superficial cortical layers and supporting stroma of the choroid plexus. Areas of positive staining on DPEAAE IHC co-localized with regions of positive staining on  $\beta$ -GAG versican IHC in the supporting stalk of the choroid plexus and in the deeper gray matter and superficial white matter layers of the developing cortex and in the white matter of the medulla at the later stages (E13.5 through E15.5) (Figures 16 and 17). Much weaker DPEAAE staining than versican staining was seen in the developing cartilage, nasal cavity, and jaw.

In the lung, anti-DPEAAE immunoreactivity was lower at E12.5 and E13.5 than at E14.5 and E15.5. At E12.5 and E13.5, there was very weak intracytoplasmic staining of the lung

mesenchyme. At E13.5, there was more pronounced DPEAAE immunoreactivity of the mesenchyme, which increased at E14.5 and E15.5, particularly around the basement membrane and the external surface of the pulmonary parenchyma, which co-localized with areas of decreased versican immunoreactivity at these ages (Figure 18). There was no significant difference in DPEAAE immunoreactivity over time in the lung.

Virtually no DPEAAE immunoreactivity was seen in adult brain, heart, lung, or liver (all tissues <0.1% ratio of positive DPEAAE expression to total tissue area).

***Versican  $\alpha$ -GAG immunohistochemistry mirrors versican V2 gene expression in the lung and head of E12.5 and E13.5 embryos.***

In the whole embryo at E12.5 and E15.5, there was less  $\alpha$ -GAG than  $\beta$ -GAG immunoreactivity (Figure 19). Consistent with results of V2 versican isoform gene expression by mRNA, there was little  $\alpha$ -GAG versican immunoreactivity in the E12.5 and E13.5 lung, with only mild positivity of the cells lining the airways (Figure 20). However, in the embryonic brain at E13.5, there was moderate to strong  $\alpha$ -GAG as well as  $\beta$ -GAG versican immunoreactivity throughout the white matter, deeper gray matter, and ventricular lining cells and cells of the choroid plexus (Figure 19; Figure 20). There was significantly higher  $\alpha$ -GAG staining in the brain compared to the liver and lung at E13.5 ( $p < 0.05$ ).

## Discussion

Similar to a previous study [31], we found that total versican gene expression by PCR is significantly higher during embryonic development than in adult tissues, and the highest total versican gene expression in the embryo occurs at day E13.5. In our study, we further investigated versican gene expression in individual organs (the liver, lung, head, and heart), and found that during embryonic development in the time period tested, these organs each have higher versican expression than the corresponding adult organ. We also examined versican expression in the embryo immunohistochemically and found that areas of versican expression in the lung and brain generally involved regions of cell proliferation and differentiation and locations of scaffolding for tissue development and migration, such as the pulmonary interstitium, the developing roof of the neopallial cortex and hindbrain, and the white matter tracts. We found that these areas of versican expression co-localized with DPEAAE expression. Similar to the adult, at the latest embryonic time point tested (E15.5), versican gene expression was lowest in the liver, highest in the brain, and intermediate in the heart and lung.

### Liver

Relative versican gene expression and versican  $\beta$ -GAG immunoreactivity in liver was low at all embryonic time points tested and decreased significantly from E11.5 to E15.5. In murine liver development, the hepatic sinusoids form from E10-E11, and from E11.5-E12.5 the liver begins to rapidly enlarge as it assumes the primary responsibility for hematopoiesis from the yolk sac [59],[62]. From E11.5-E15, the liver markedly expands and contains a greater proportion of hepatic parenchyma and fewer sinusoids [59],[62]. At E15.5, the primary site of

hematopoiesis for erythroid and myelolymphoid precursors shifts to the spleen [62]. This change in liver function relative to hematopoiesis and expansion of the hepatic parenchyma with relative decrease in the sinusoids at E11.5 likely explains the subsequent decrease in versican throughout liver development.

### Heart

In mice, the heart is the first organ to develop, with formation of paired cardiogenic plates at E7.5 and a rudimentary circulatory system in place by E8.5-E9 [59],[63]. Differentiation of the outflow tract and the aortico-pulmonary spiral septum occurs at E10-E11, development of aortic arch occurs at E12, and between E13 and E14 the aorta separates from the pulmonary tract, interatrial and interventricular septation progresses, and the cardiac valves appear and develop [59],[63]. By E15.5, the cardiovascular system has essentially completed its prenatal structure [59],[63]. Versican gene expression previously has been shown to occur at high levels during cardiac development [37]. Versican expression has been detected immunohistochemically in the endocardial cushions of the AV canal, the outflow tract, the aortic sac, and the ventricular subendocardium; however, little versican expression is reported in the myocardium [37],[50]. At E11.5, we found that the highest versican gene expression by versican copy number of all the organs tested was in the heart, and we found that versican gene expression in the total embryonic heart by mRNA was higher than that in the adult heart at every time point tested. In our study, relative versican gene expression in the heart was higher during the early time points of gestation (E11.5 - E13.5) and subsequently decreased in the heart at E14.5 and E15.5. E11.5 to E13.5 is a time of critical differentiation of the cardiac vasculature and formation and remodeling of the atrioventricular cushions, which requires an epithelial to

mesenchymal transition [63]. Versican deposition and proteolysis most likely has an important role mediating cellular proliferation, the epithelial-mesenchymal transition, and migration of cells through a developmental scaffold [12],[50],[59].

Given the strong body of literature regarding versican isoform gene expression and immunohistochemistry in the heart, we chose to limit further investigation of versican isoform expression and versican and DPEAEE immunohistochemical analysis to the central nervous system (brain) and the lung.

### Brain

In murine nervous system development, the forebrain, midbrain, and hindbrain vesicles form at E8.0, and division of the forebrain vesicle to form the third ventricle and telencephalic vesicles occurs at E9, with subsequent differentiation of the telencephalic vesicles from E10-11 [59]. At E12, hypothalamic, thalamic, and otocyst differentiation and expansion of the corpus striatum occurs, and the 3rd ventricle decreases in size [59]. The choroid plexus first appears at E12.5-E13.0, and expansion of the neopallial cortex and differentiation of the olfactory lobes and pituitary gland occurs from E12.5 to E14, with stratification of the neopallial cortex to form the primary cortex at E14 [59]. At E15, pronounced differentiation of the cerebellar primordium and olfactory lobes is apparent and the olfactory lobes become lined by olfactory epithelium [59]. In our study, versican gene expression in the head was significantly higher at E13.5, at the time of neopallial cortex and olfactory lobe expansion and differentiation, compared to earlier embryonic ages. Relative ADAMTS-1 gene expression in embryonic head showed a similar pattern to versican gene expression, although differences in relative ADAMTS-1 gene expression at the

various embryonic ages were not statistically significant. Previous studies have demonstrated strong ADAMTS-5 and transient and more limited ADAMTS-9 expression in the embryonic brain; these were not investigated in the present study [40],[64].

On immunohistochemistry, versican immunoreactivity was most pronounced in the white matter and in the roof of the neopallial cortex and midbrain at all ages, with the strongest positive versican  $\beta$ -GAG staining noted at E13.5 and later, consistent with our mRNA results. Staining decreased in intensity at E14.5 and E15.5 compared to E13.5, but increased in extent. Areas of positive staining on versican  $\beta$ -GAG immunohistochemistry co-localized with areas of anti-DPEAAE staining. A previous study performed in the rat at E16 showed versican  $\alpha$ -GAG and  $\beta$ -GAG immunoreactivity in the marginal zone of the cerebral cortex, internal capsule, and optic and olfactory tracts [35]. Similar to these findings, at later ages (E13.5, E14.5, and E15.5) we noted  $\beta$ -GAG versican immunopositivity of the marginal zone of the neopallial cortex, roof of the midbrain, cerebellar primordium, and developing olfactory lobe. At later ages (E14.5 and E15.5), we also noted increased DPEAAE staining in the white matter and superficial cortical layers, which co-localized with regions of positive  $\beta$ -GAG versican staining in the deeper gray matter and superficial white matter layers of the developing cortex and in the white matter of the medulla. In other regions of the embryonic brain, such as the periventricular gray and adjacent white matter, positive  $\beta$ -GAG versican staining co-localized with areas of negative DPEAAE staining. Patterns of positive staining on quantitative DPEAAE immunohistochemistry for the brain were the inverse of  $\beta$ -GAG versican staining. These results suggest complementary but antagonistic roles of versican and versican degradation during embryogenesis of the central nervous system, with proteoglycans such as versican potentially facilitating cell growth and

mediating cell migration through a provisional extracellular matrix, as has been previously proposed to occur in lung and musculoskeletal development and in lung inflammation [22], [46],[65],[66]. Degradation of versican may occur to limit further migration and cellular differentiation once the process is complete. In the brain,  $\alpha$ -GAG immunoreactivity increased towards later gestational ages and in adult controls, consistent with a significant increase in V2 versican isoform mRNA expression in later gestation, which also suggests a switch towards inhibition of neural proliferation and outgrowth in later embryonic development [10],[13],[14].

One drawback of the current study is that versican gene expression in the embryonic head was used as an estimate of gene expression in the brain, given the difficulty of removing the brains from the calvaria at the earlier time points. Therefore, some developing bone and skin was analyzed in addition to the nervous tissue. Previous studies in humans have shown high versican expression in fetal skin which may have affected our results [17]. On our quantitative immunohistochemistry analysis, we measured head and brain separately and found a similar pattern for all of the embryonic ages studied, although versican immunoreactivity was consistently less for the brain than for the whole head. We feel that embryonic head serves as a reasonable approximation of embryonic brain for our mRNA data.

### Lung

In mice, lung development begins at E 9.5, with lung buds sprouting from the foregut tube [39],[59]. From E10 to E11, the lung buds extend from the ventral aspect of the developing esophagus into the pericardio-peritoneal canals, and by E12 primary and secondary bronchi have developed [59]. At E13, pulmonary arteries enter the lung buds, lobation of the right lung occurs, and the epithelial lining of the lower airways first appears. From E13 to E14, splanchnic

mesenchyme condenses in anticipation of subsequent differentiation of the connective tissue, smooth muscle, and cartilage of upper airways. Primary, secondary and tertiary bronchi are apparent with differentiation of the terminal bronchi and bronchioles by E15 [59]. From E14.5 to E16, there is a pronounced increase in bronchioles per region of lung [59].

We showed maximum versican expression in embryonic lung at E13.5, at the time of pulmonary vascularization, lung lobation, and airway epithelialization, with a subsequent decline at later embryonic ages, consistent with results of previous studies in mice and sheep [3],[39]. We also saw strong versican  $\beta$ -GAG immunoreactivity at all ages examined throughout the mesenchyme of the developing lung with pronounced positive staining of the basement membrane of airways but little to no positive staining of the airway epithelium. These findings suggest a role of versican in development of the lung vasculature and expansion of the alveolar space. In our study, versican  $\beta$ -GAG immunoreactivity was significantly higher in E13.5 lung compared to E11.5 lung and also appeared to decrease in later gestation. At E14.5 and E15.5, there was reduced  $\beta$ -GAG immunoreactivity around the airways and along the periphery of the lung, which co-localized with areas of increased positivity on DPEAAE staining and suggests degradation of versican in these regions once cell proliferation, differentiation, and migration has occurred. Patterns of positive staining on quantitative DPEAAE immunohistochemistry for the lung, as in the brain, were the inverse of  $\beta$ -GAG versican staining, suggesting antagonistic roles of versican deposition and versican proteolysis in promoting and inhibiting cellular proliferation, adhesion, and migration through a provisional extracellular matrix during development, as has been previously proposed during embryonic development for the musculoskeletal system and heart [46],[50],[66]. As in the brain, versican appears to be important for lung development in

mediating epithelial-mesenchymal interactions and providing an extracellular matrix rich in growth factors which acts to regulate cell adhesion and proliferation [12],[18],[65].

In our study, ADAMTS-1 gene expression in the fetal lung was much lower than in adult lung at all of the time points tested, which is not consistent with a previous report of ADAMTS1 expression during murine development [53]. The *Ct* values for the embryo lung ADAMTS1 samples were similar to those for the other organs in our study, but the *Ct* values for the adult lung samples were very low, and we would need to repeat the PCR study on other adult lung samples to verify this unexpected finding. Strong expression of ADAMTS-9 in the mesenchyme of the lung from E14.5 to E17.5 has also been previously shown, which was not investigated in the current study [64]. We focused on ADAMTS-1 expression because it was reported in the literature to be one of the most widely expressed ADAMTS proteinases during embryonic development; however, investigation of the relative gene expression of single ADAMTS proteases during organ development may not be biologically relevant. Evidence from previous studies suggests that redundancy or compensation for missing or deficient ADAMTS proteases may occur [57],[58].

In this project, versican accumulation was measured by immunohistochemistry using the  $\beta$ -GAG antibody. The anti- $\beta$ -GAG antibody mainly reacts to VO and V1; whereas the anti- $\alpha$ -GAG antibody mainly reacts to V2 [10],[35]. In adults, low levels of  $\beta$ -GAG versican are present in health, and versican increases in the lung and other organs following injury and in many types of neoplasia [1],[6],[25],[28],[29],[44]. Alpha-GAG versican, in contrast, is normally present throughout the postnatal and adult period in the central nervous system [10]. Limited immunohistochemistry in the present study using the  $\alpha$ -GAG antibody was performed,

which showed substantially less  $\alpha$ -GAG than  $\beta$ -GAG immunoreactivity at E12.5 and E13.5 in most tissues, consistent with our findings of little V2 versican isoform gene expression in the embryonic head, heart, liver, and lung. However,  $\alpha$ -GAG immunoreactivity and V2 versican isoform mRNA expression were detected in the embryonic brain at E13.5 and later stages of gestation, consistent with development of a more adult versican isoform profile in the brain.

Limitations of this study include relatively small sample sizes and differences in organ analysis between embryos and adults. The use of larger embryonic litter sizes may have resulted in more statistically significant trends over time for versican gene expression and quantitative immunohistochemistry in the organs tested. Another limitation is that the entire embryonic organ was used for gene expression assays, and organs from littermates were pooled, while a representative portion of the organ was used from the adult. This may have led to discrepancies in versican content depending on organ location sampled, especially for less homogenous organs such as the heart and the brain. Nevertheless, the findings of this study suggest that versican deposition and proteolysis is important in embryonic development of the lung and brain from E11.5 to E15.5 in the mouse. This study advances the literature by providing a comprehensive investigation of versican isoform mRNA expression, versican  $\beta$ -GAG immunoreactivity, and DPEAAE immunoreactivity in the brain and the lung of the mouse during mid to late gestation.

## Conclusions

Consistent with its putative role in cell proliferation and migration during development, we found significantly increased levels of versican gene expression and  $\beta$ -GAG immunoreactivity in the embryonic head and lung compared to adult controls. Versican expression was highest at E13.5 in the lung and the brain, an embryonic age in the mouse associated with rapid expansion and differentiation of these two organs. Versican degradation as measured by DPEAAE immunoreactivity tended to inversely mirror versican  $\beta$ -GAG immunoreactivity in these organs and increased at the later gestational ages, following the peak versican expression at E13.5. There was a more adult profile of versican gene expression in the various organs at the last gestational time point tested, consistent with a decrease in cell proliferation, differentiation, and migration in later gestation following organogenesis.

**Figure 1.** Versican has 4 different isoforms: V0, V1, V2, and V3. The structure of versican isoform, V0, is characterized by an approximately 550 kDa core protein consisting of an amino-terminal (G1) domain which binds hyaluronan and a carboxy-terminal (G3) domain, as well as two central chondroitin sulfate glycosaminoglycan attachment domains, the  $\alpha$ -GAG and  $\beta$ -GAG domains. The immunohistochemical staining properties using antibodies specific to the  $\alpha$ -GAG and  $\beta$ -GAG domains allow for the identification of the versican isoforms in tissues. Figure courtesy of Charles W. Frevort.

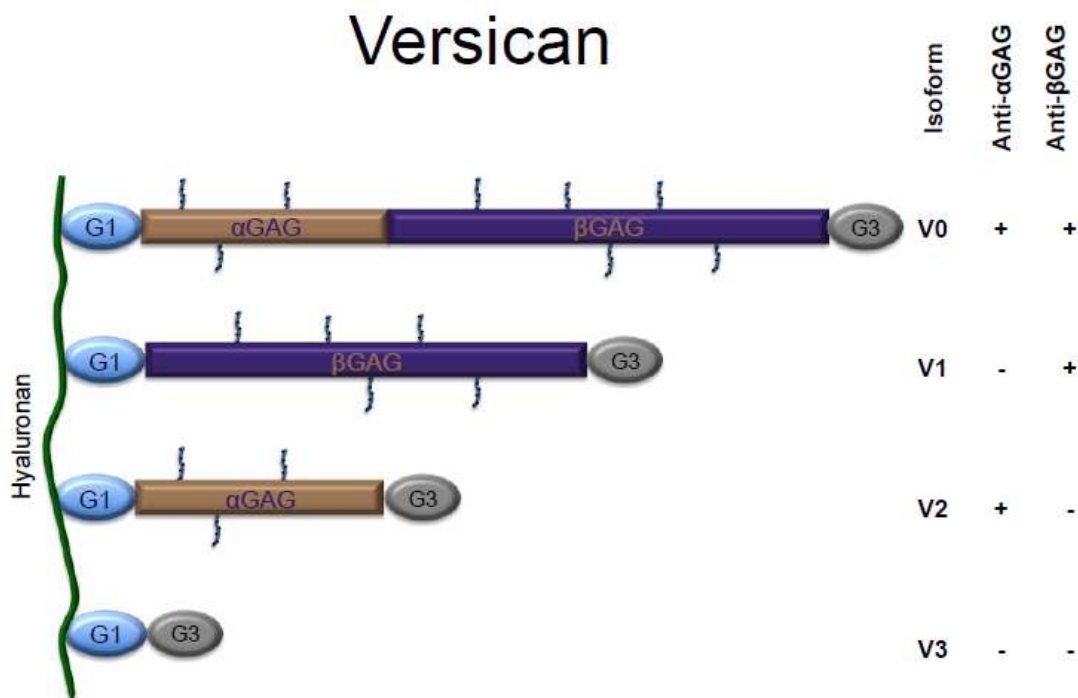


**Figure 2.** Positive staining (brown) for the  $\beta$ -GAG domain of versican in E11.5 (left) and E14.5 (right) embryonic tissue with hematoxylin counter stain (blue). Sample images of regions of interest (ROIs) manually drawn around the organs measured using the Visiopharm Image Analysis module.

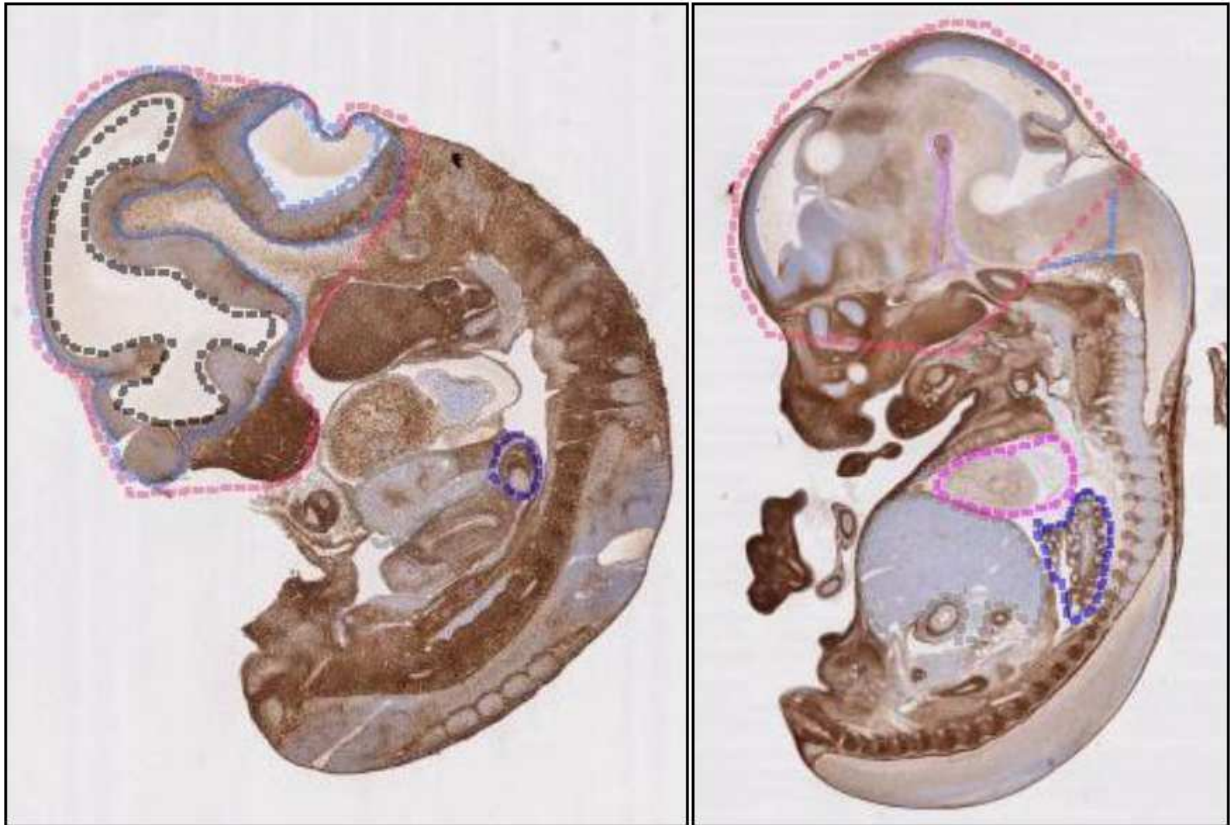


**Figure 3. Cumulative versican gene expression by embryonic day is highest at E13.5.**

Contribution to the total embryonic gene expression by versican copy number in the lung, liver, heart, and brain is shown at E11.5, E12.5, E13.5, E14.5, E15.5, and in the adult control. Changes in the amounts of mRNA for versican were determined using mRNA collected from embryonic organ homogenates and quantitative real time PCR. A versican standard curve was constructed using the versican V3 plasmid (mouse) total versican standard relating *Ct* value for 15ng cDNA to versican copy number.

### Cumulative Versican Expression by Embryonic Day

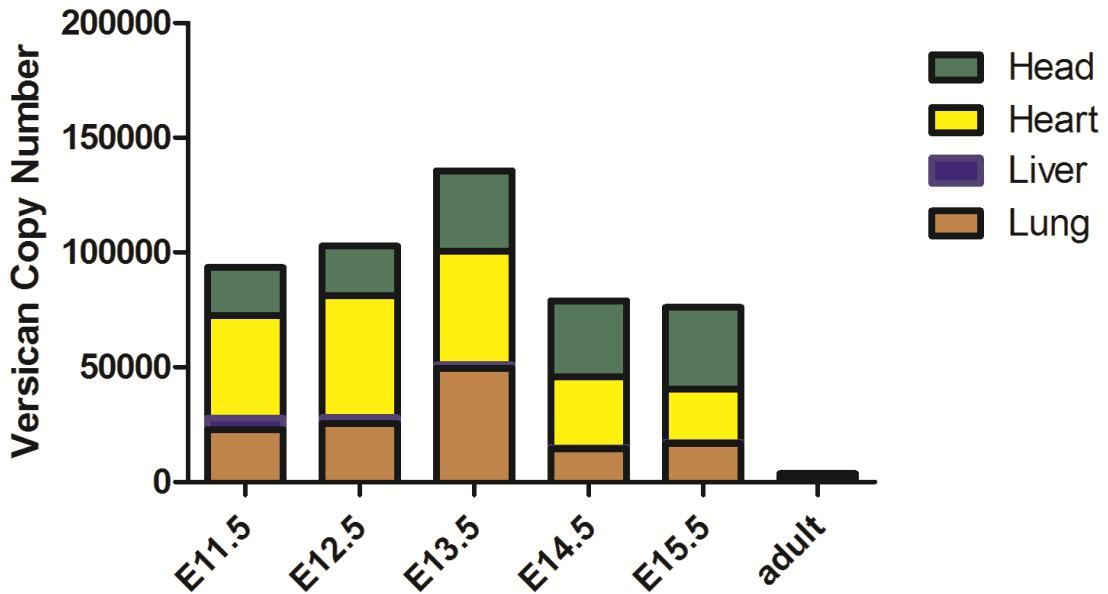


**Figure 4. The V0 and V1 versican isoforms predominate in embryonic head and lung from E11.5 to E15.5.** Changes in the relative amounts of mRNA for the four versican isoforms were determined using mRNA collected from embryonic organ homogenates and quantitative real time PCR. Values are the mean  $\pm$  SEM with a minimum n=3 for each group studied. The expression of mRNA for the versican isoforms in the embryonic head (top) and lung (bottom) is expressed as a relative fold increase in mRNA over the adult control.

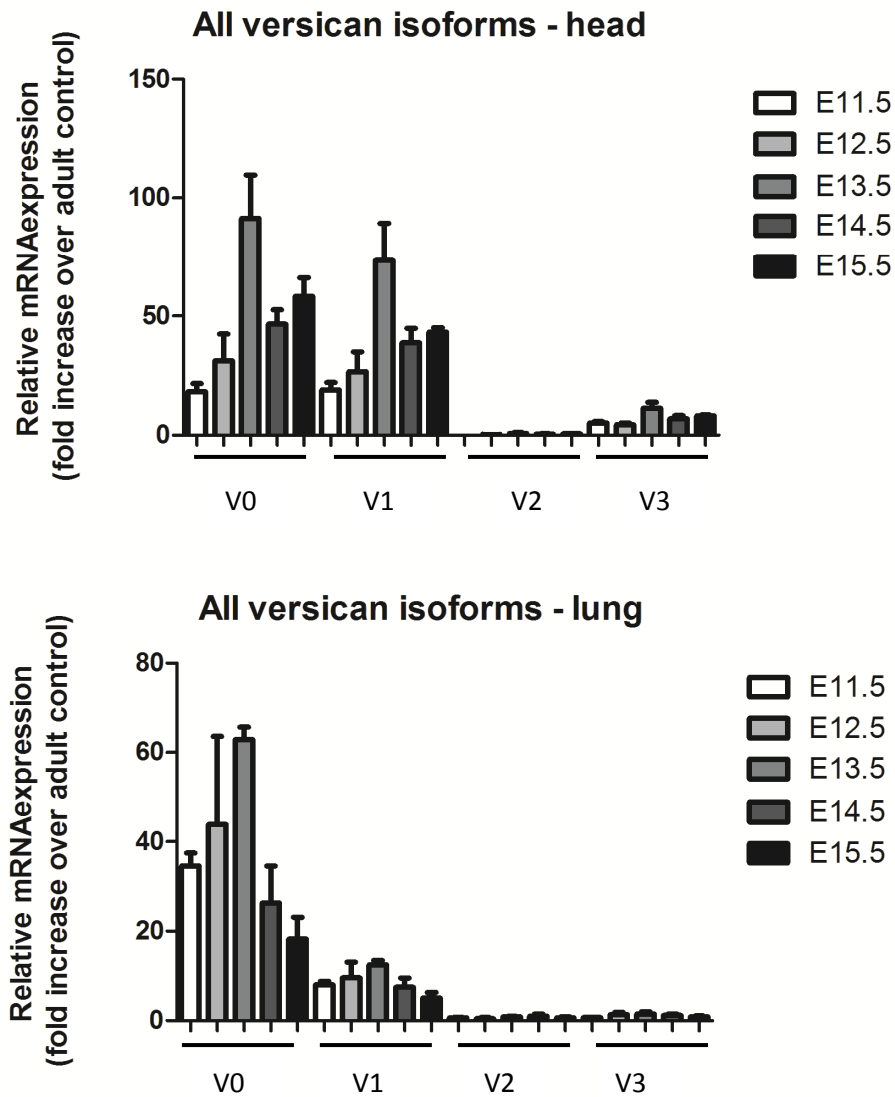


**Figure 5. The V2 versican isoform increases in embryonic head but not lung at E13.5.**

Changes in the relative amounts of mRNA for the V2 versican isoform were determined using mRNA collected from embryonic organ homogenates and quantitative real time PCR. Values are the mean  $\pm$  SEM with a minimum n=3 for each group studied. The expression of mRNA for the V2 versican isoform in the embryonic head (top) and lung (bottom) is expressed as a relative fold increase in mRNA over the adult control. An asterisk (\*) shows groups that are significantly different ( $p < 0.05$ ).

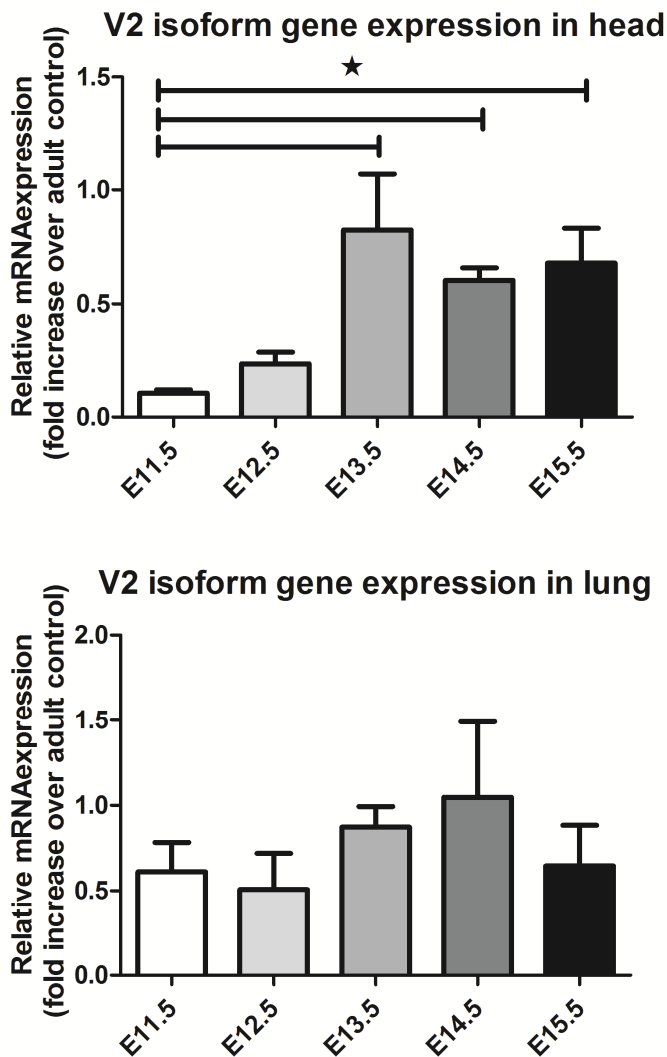


**Figure 6.** Representative E11.5 embryo on  $\beta$ -GAG immunohistochemistry, identifying key anatomic structures. Positive staining for  $\beta$ -GAG is brown with a hematoxylin counterstain (blue).

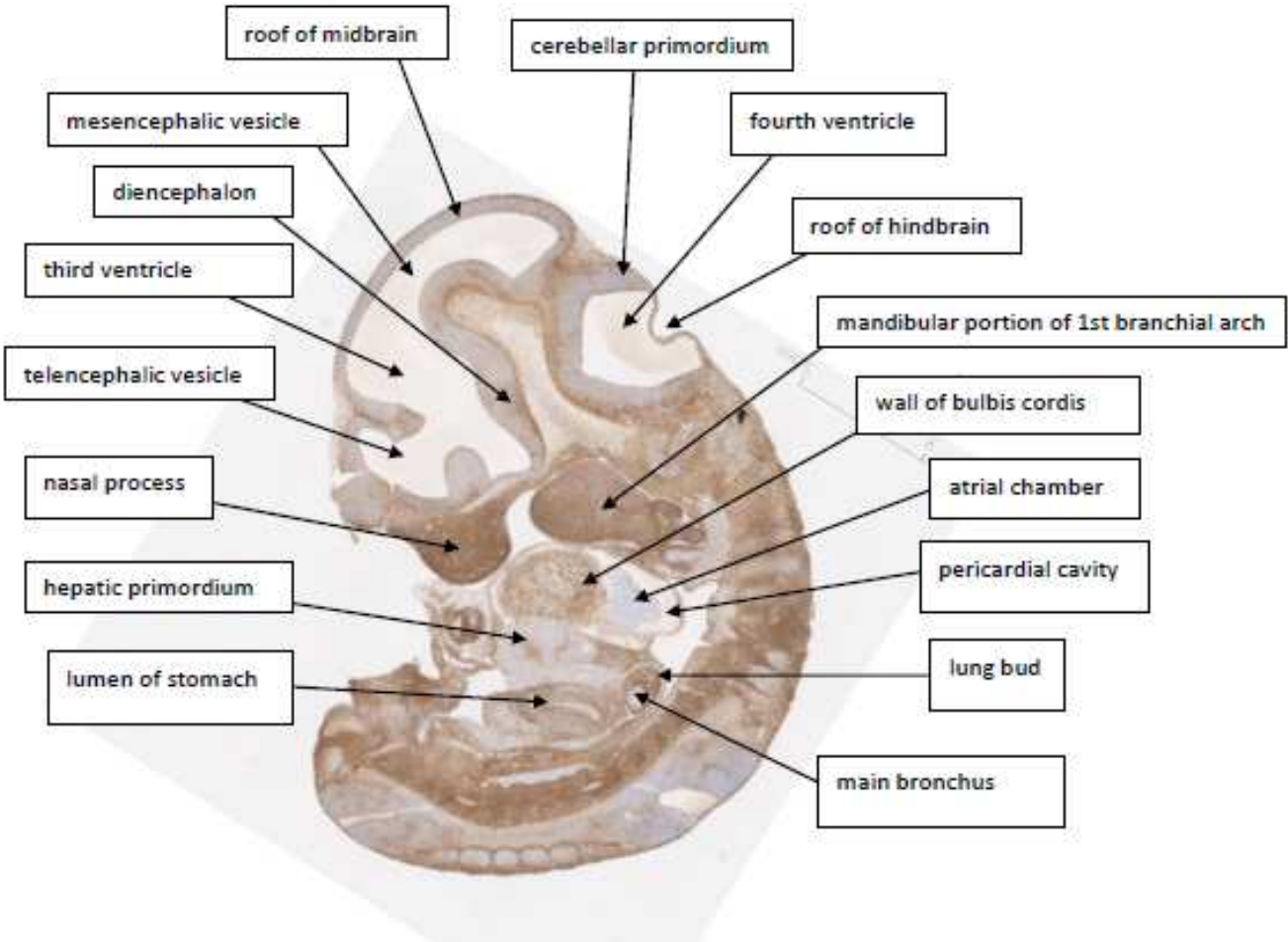


**Figure 7.** Representative E12.5 embryo on  $\beta$ -GAG immunohistochemistry, identifying key anatomic structures. Positive staining for  $\beta$ -GAG is brown with a hematoxylin counterstain (blue).

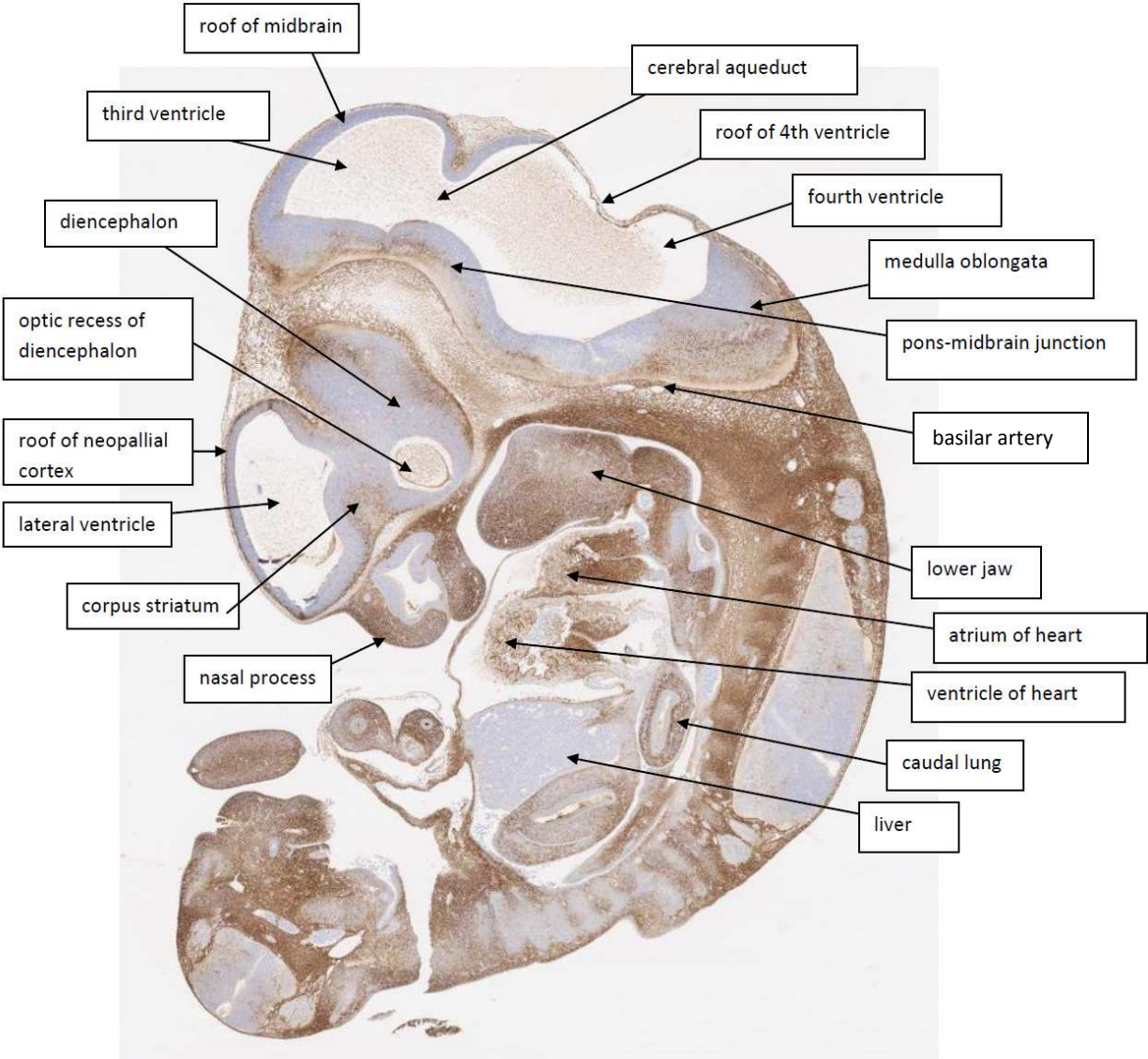


**Figure 8.** Representative E13.5 embryo on  $\beta$ -GAG immunohistochemistry, identifying key anatomic structures. Positive staining for  $\beta$ -GAG is brown with a hematoxylin counterstain (blue).

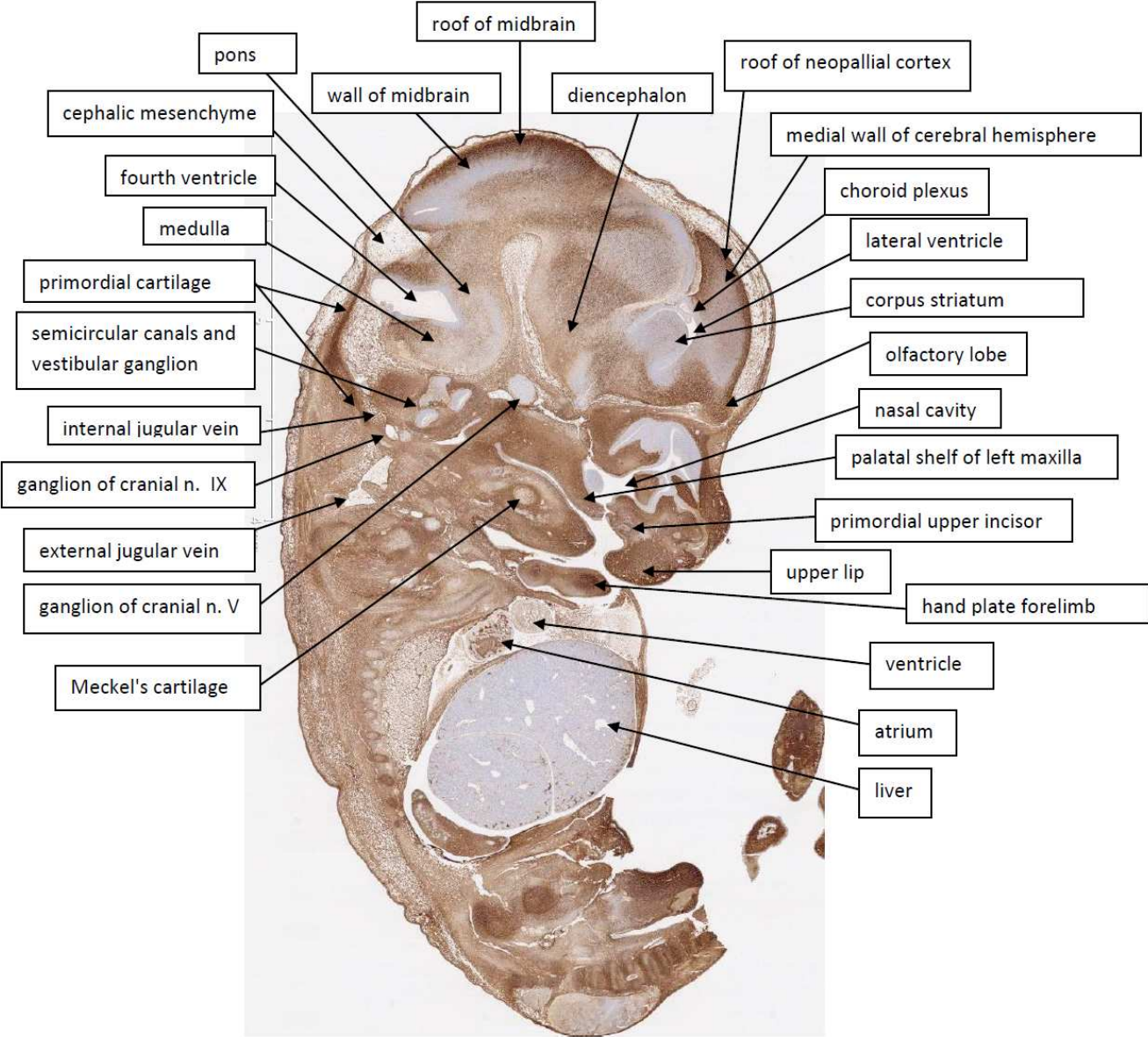


**Figure 9.** Representative E14.5 embryo on  $\beta$ -GAG immunohistochemistry, identifying key anatomic structures. Positive staining for  $\beta$ -GAG is brown with a hematoxylin counterstain (blue).

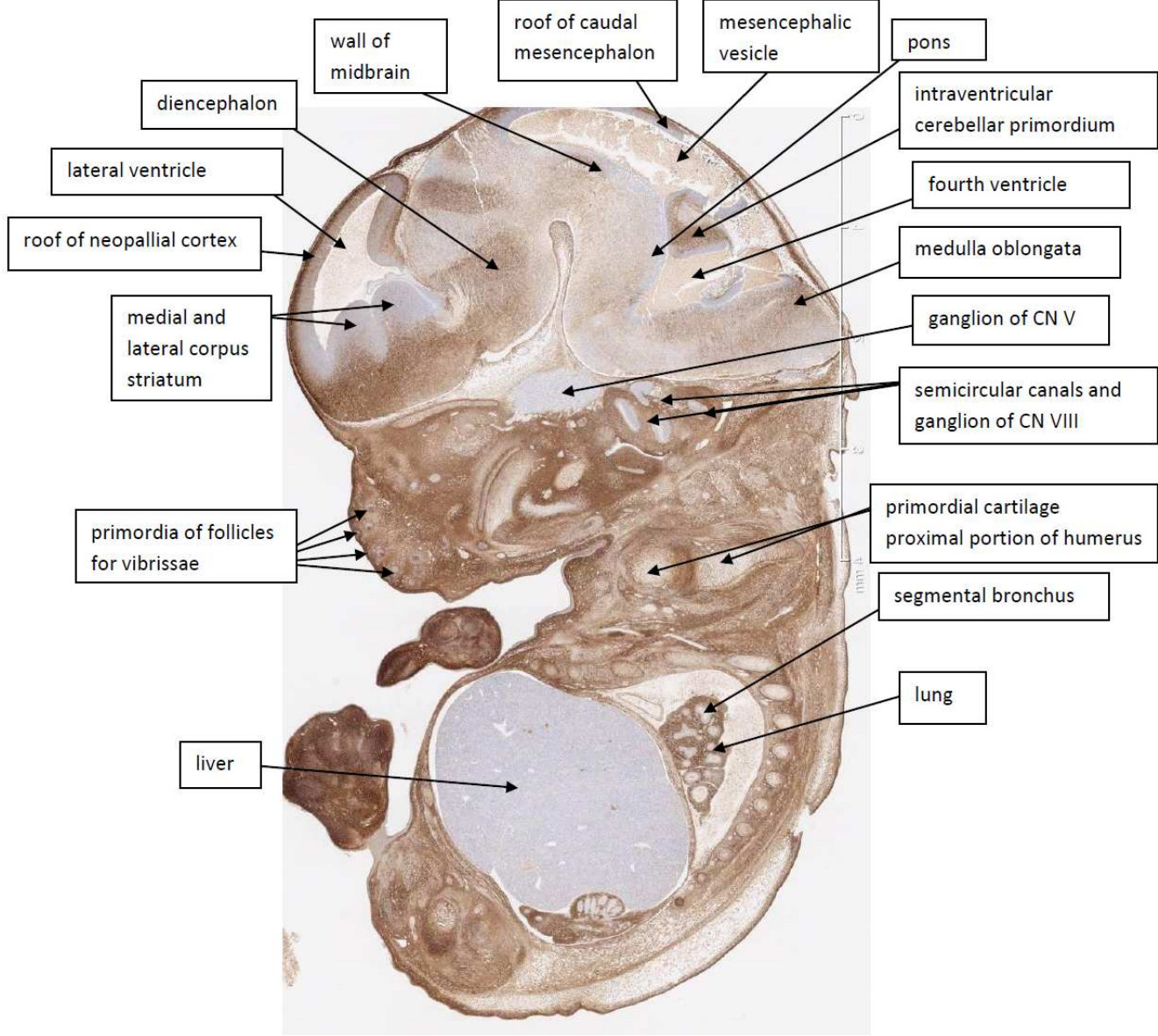


**Figure 10.** Representative E15.5 embryo on  $\beta$ -GAG immunohistochemistry, identifying key anatomic structures. Positive staining for  $\beta$ -GAG is brown with a hematoxylin counterstain (blue).

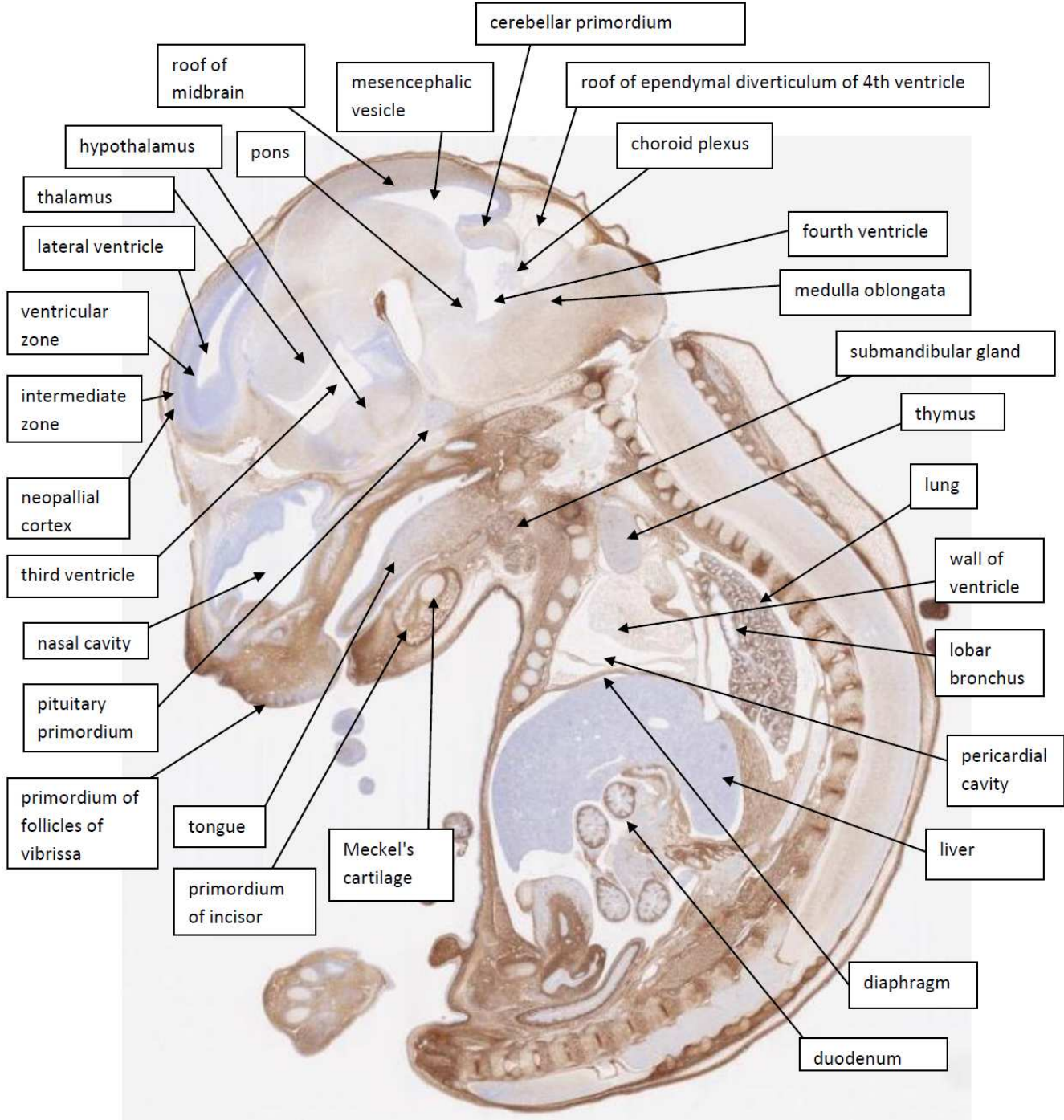


**Figure 11. Versican expression in embryonic lung is maximal at E13.5.** Top panel: Versican  $\beta$ -GAG quantitative immunohistochemistry (left) and relative gene expression (right) in embryonic lung over 5 embryonic ages. Bottom panel: Versican  $\beta$ -GAG immunohistochemistry at E11.5 (A, 17.5x magnification); E13.5 (B, 20x); and E15.5 (C, 19x). Positive immunostaining for versican is brown with hematoxylin used as a counter stain (blue). Changes in the versican IHC were determined by calculating ratio of versican to total tissue area using the visiofarm image analysis module. Changes in relative amounts of mRNA for versican were determined using mRNA collected from embryonic organ homogenates and quantitative real time PCR. Values are the mean  $\pm$  SEM with a minimum n=3 for each group studied. The expression of mRNA for versican is expressed as a relative fold increase in mRNA over the adult control. An asterisk (\*) shows groups that are significantly different ( $p < 0.05$ ).

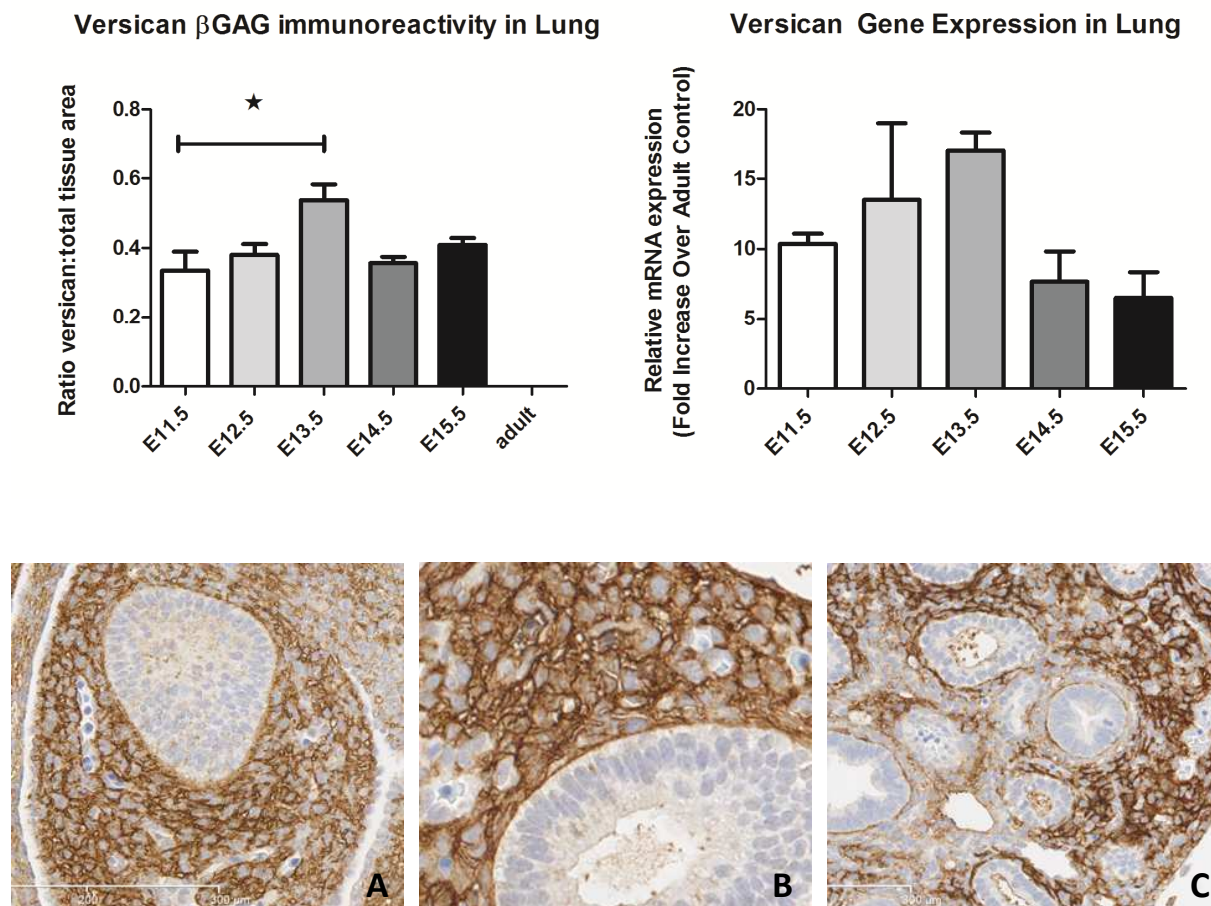


**Figure 12. Versican expression in embryonic liver decreases from E11.5 to E15.5.** Top panel: Versican  $\beta$ -GAG quantitative immunohistochemistry (left) and relative gene expression (right) in embryonic liver over 5 embryonic ages. Bottom panel: Versican  $\beta$ -GAG immunohistochemistry at E11.5 (A, 20x magnification); E13.5 (B, 10x); and E15.5 (C, 20x). Positive immunostaining for versican is brown with hematoxylin used as a counter stain (blue). Changes in the versican IHC were determined by calculating ratio of versican to total tissue area using the visiofarm image analysis module. Changes in relative amounts of mRNA for versican were determined using mRNA collected from embryonic organ homogenates and quantitative real time PCR. Values are the mean  $\pm$  SEM with a minimum n=3 for each group studied. The expression of mRNA for versican is expressed as a relative fold increase in mRNA over the adult control. An asterisk (\*) shows groups that are significantly different ( $p < 0.05$ ).

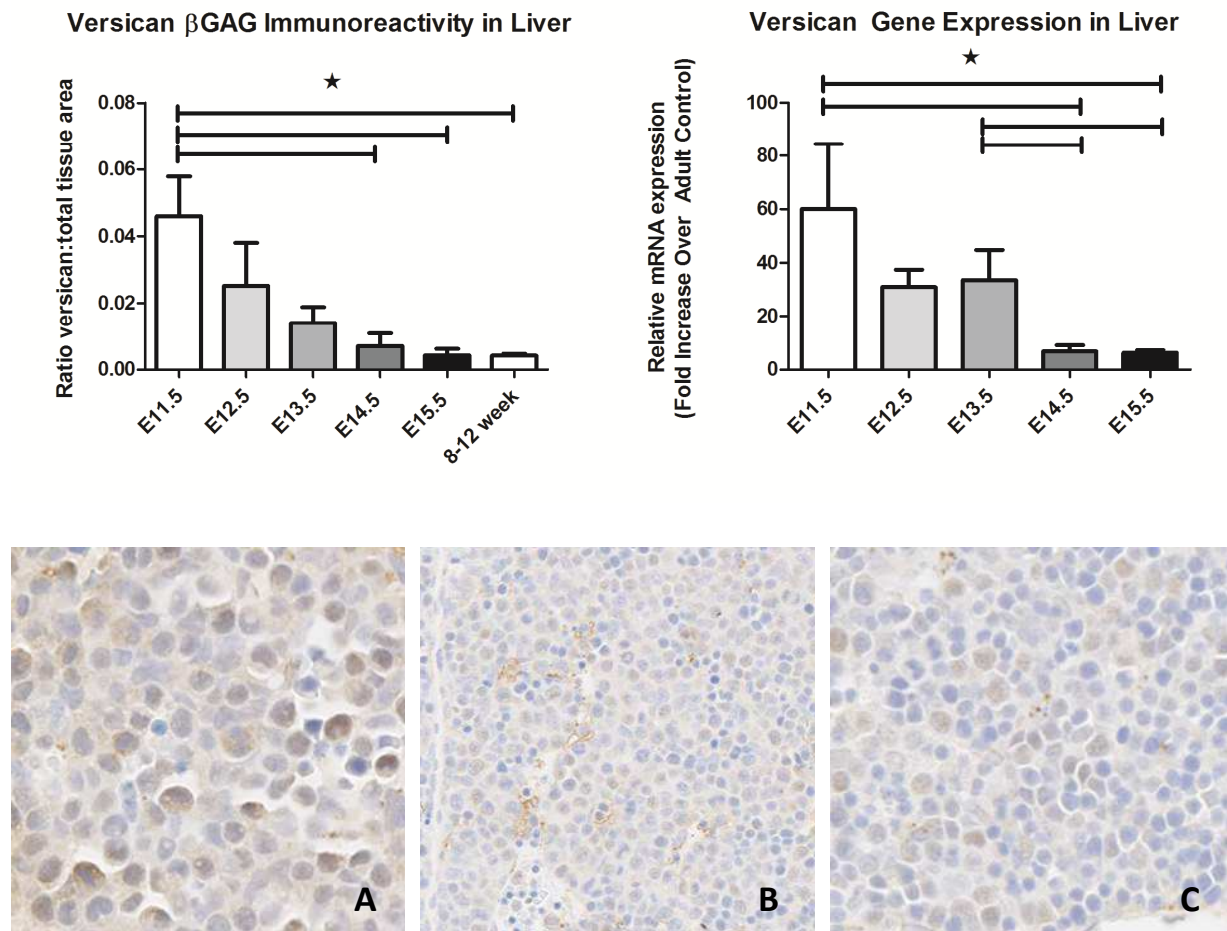
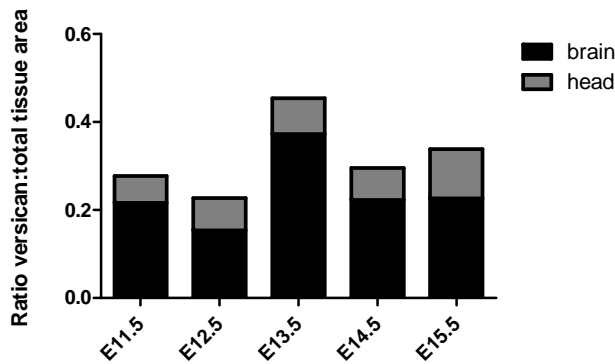


**Figure 13. There is higher  $\beta$ -GAG immunoreactivity in embryonic head than brain, although the pattern of positive staining is similar in both regions, and versican  $\beta$ -GAG immunoreactivity in the embryonic brain is significantly higher than in the adult control.**

Top: Quantitative versican  $\beta$ -GAG immunohistochemistry in brain versus head at five embryonic ages. Bottom: Versican  $\beta$ -GAG immunoreactivity over time at five embryonic ages and in adult control brain. Changes in the  $\beta$ -GAG versican quantitative immunohistochemistry were determined by calculating ratio of versican to total tissue area using the visiopharm image analysis module. Values are the mean  $\pm$  SEM with a minimum n=3 for each group studied. An asterisk (\*) shows groups that are significantly different ( $p < 0.05$ ).

**Versican  $\beta$ -GAG immunoreactivity in embryonic brain versus head**



**Versican  $\beta$ -GAG Immunoreactivity in Brain**

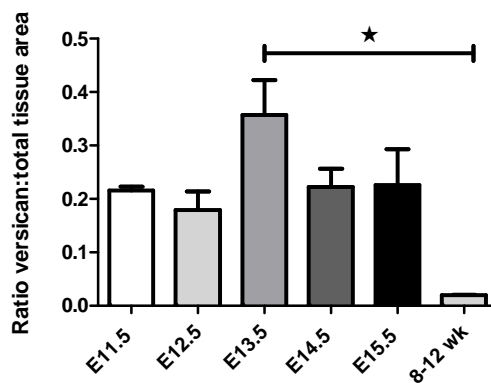


**Figure 14. Versican expression in embryonic head is maximal at E13.5.** Top panel: Versican  $\beta$ -GAG quantitative immunohistochemistry (left) and relative gene expression (right) in embryonic head over 5 embryonic ages. Bottom panel: Versican  $\beta$ -GAG immunohistochemistry at E11.5 (A, image at 5x); E13.5 (B, image at 1.25x); and E15.5 (C, image at 1.25x). Positive immunostaining for versican is brown with hematoxylin used as a counter stain (blue). Changes in the versican IHC were determined by calculating ratio of versican to total tissue area using the visiopharm image analysis module. Changes in relative amounts of mRNA for versican were determined using mRNA collected from embryonic organ homogenates and quantitative real time PCR. Values are the mean  $\pm$  SEM with a minimum n=3 for each group studied. The expression of mRNA for versican is expressed as a relative fold increase in mRNA over the adult control. An asterisk (\*) shows groups that are significantly different ( $p < 0.05$ ).

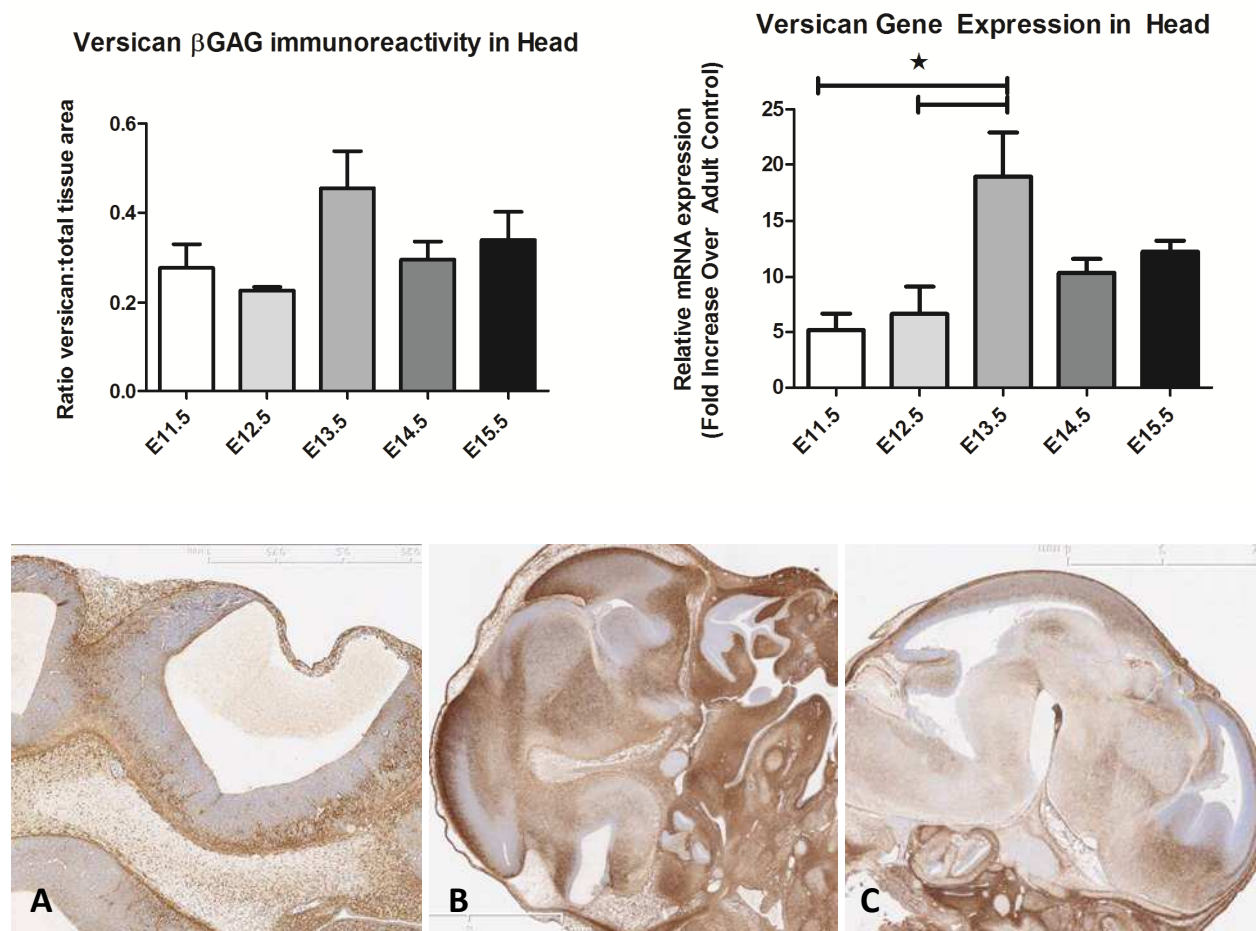
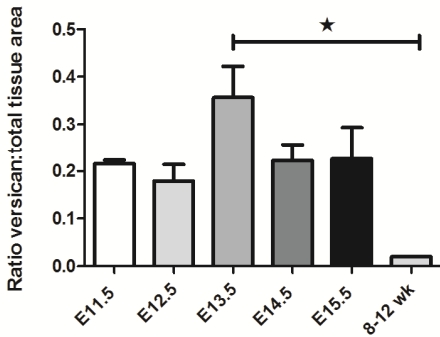
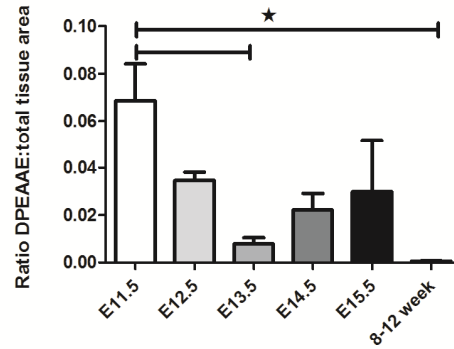


**Figure 15. There is an inverse pattern of staining on  $\beta$ -GAG versican and DPEAAE quantitative immunohistochemistry for both the lung and the head during embryonic development.** Patterns of positive staining on quantitative immunohistochemistry for versican  $\beta$ -GAG (upper left) and DPEAAE (upper right) immunoreactivity for embryonic brain (upper panel) and for versican  $\beta$ -GAG (lower left) and DPEAAE (lower right) immunoreactivity for embryonic lung (lower panel). Changes in  $\beta$ -GAG versican and DPEAAE quantitative immunohistochemistry were determined by calculating the ratios of versican and DPEAAE to total tissue area using the visiopharm image analysis module. Values are the mean  $\pm$  SEM. An asterisk (\*) shows groups that are significantly different ( $p < 0.05$ ).

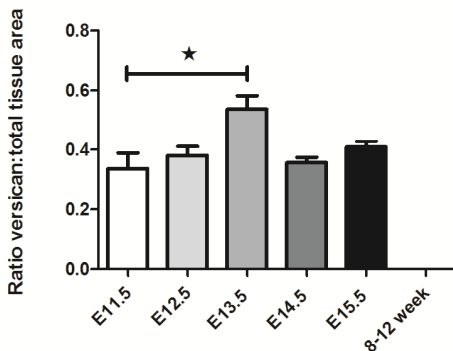
**Versican  $\beta$ -GAG Immunoreactivity in Brain**



**DPEAAE Immunoreactivity in Brain**



**Versican  $\beta$ -GAG Immunoreactivity in Lung**



**DPAEE Immunoreactivity in Lung**

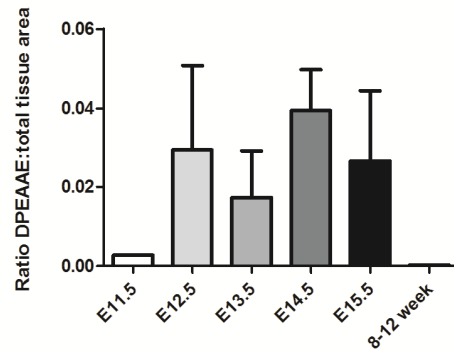


**Figure 16. There is abundant positive staining for  $\beta$ -GAG versican but sparse positive staining on DPEAAE at E13.5 in the developing neopallial cortex. A. Versican IHC.**

Positive staining for  $\beta$ -GAG versican is brown with hematoxylin used as a counterstain (blue); B. DPEAAE IHC. Positive staining for DPEAAE is brown with hematoxylin used as a counterstain (blue). Both images at 5x magnification.

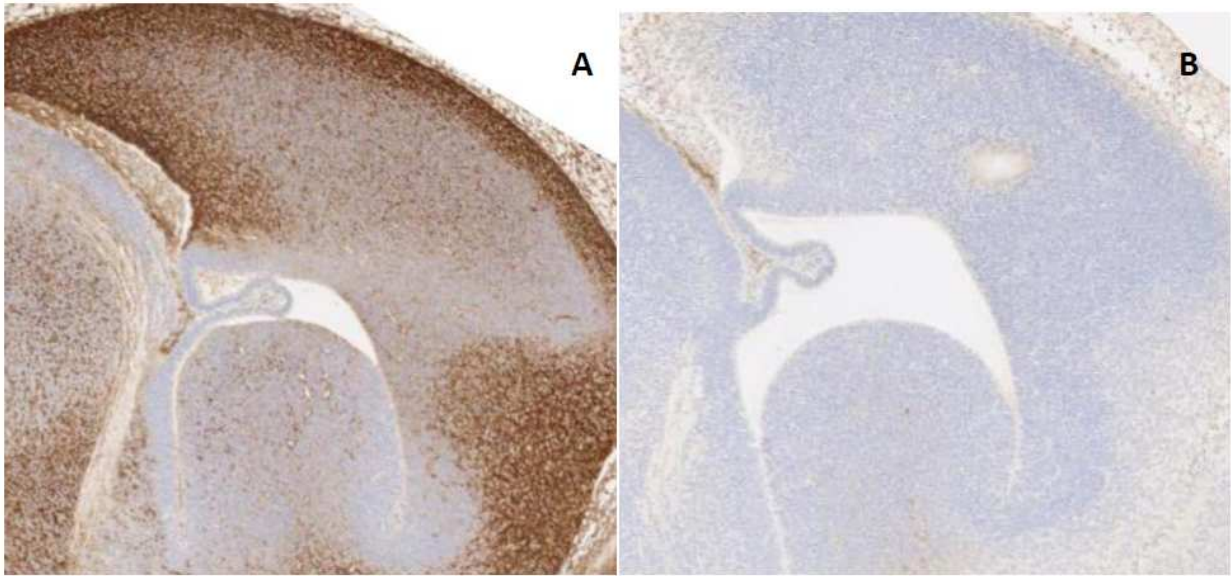


**Figure 17. Areas of staining in the embryonic brain on versican and DPEAAE immunohistochemistry colocalize.** E15.5 cerebral cortex (A and B) and medulla (C and D). A and C:  $\beta$ -GAG versican IHC; B and D: DPEAAE IHC. Positive staining for  $\beta$ -GAG versican and DPEAAE is brown with hematoxylin used as a counterstain (blue). In some regions on DPEAAE IHC, areas that stain strongly on versican IHC are positive, such as the white matter of the corpus striatum and the medulla (black arrows). In other areas of versican positivity, such as surrounding the lateral and fourth ventricle, there is weak DPEAAE immunoreactivity (white arrows). All images at 5x magnification.

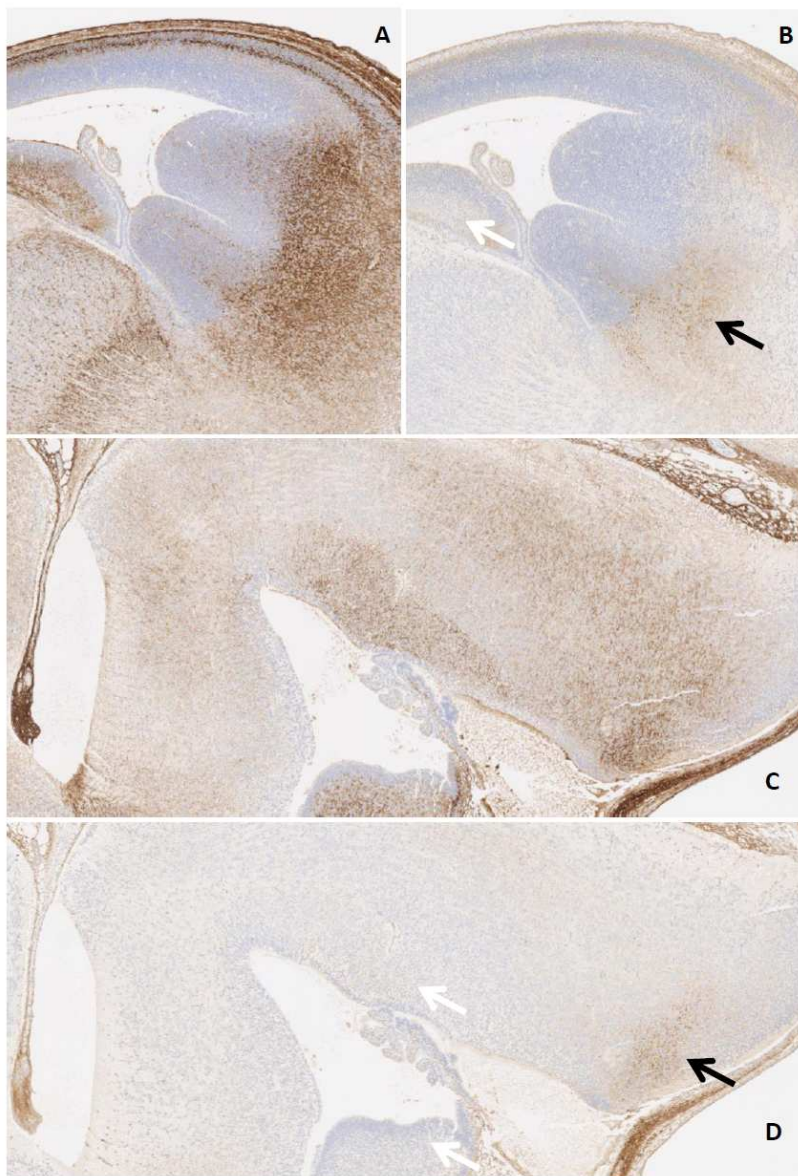


**Figure 18. Areas of staining in the embryonic lung on versican and DPEAAE immunohistochemistry colocalize.** A. E13.5 Versican  $\beta$ -GAG IHC (40x magnification); B. E13.5 DPEAAE IHC (40x); C. E15.5 Versican  $\beta$ -GAG IHC (20x); D. E15.5 DPEAAE IHC (20x). There is strong homogeneous versican staining of the mesenchyme at E13.5 (A,B) and little DPEAAE staining at this age. At E15.5 (C,D), areas of negative staining on versican IHC (white arrows) at the periphery of the lung and surrounding the airways correspond to areas of positive staining on DPEAAE IHC (dark arrows). Positive staining for versican  $\beta$ -GAG and DPEAAE is brown, with hematoxylin used as a counterstain (blue).

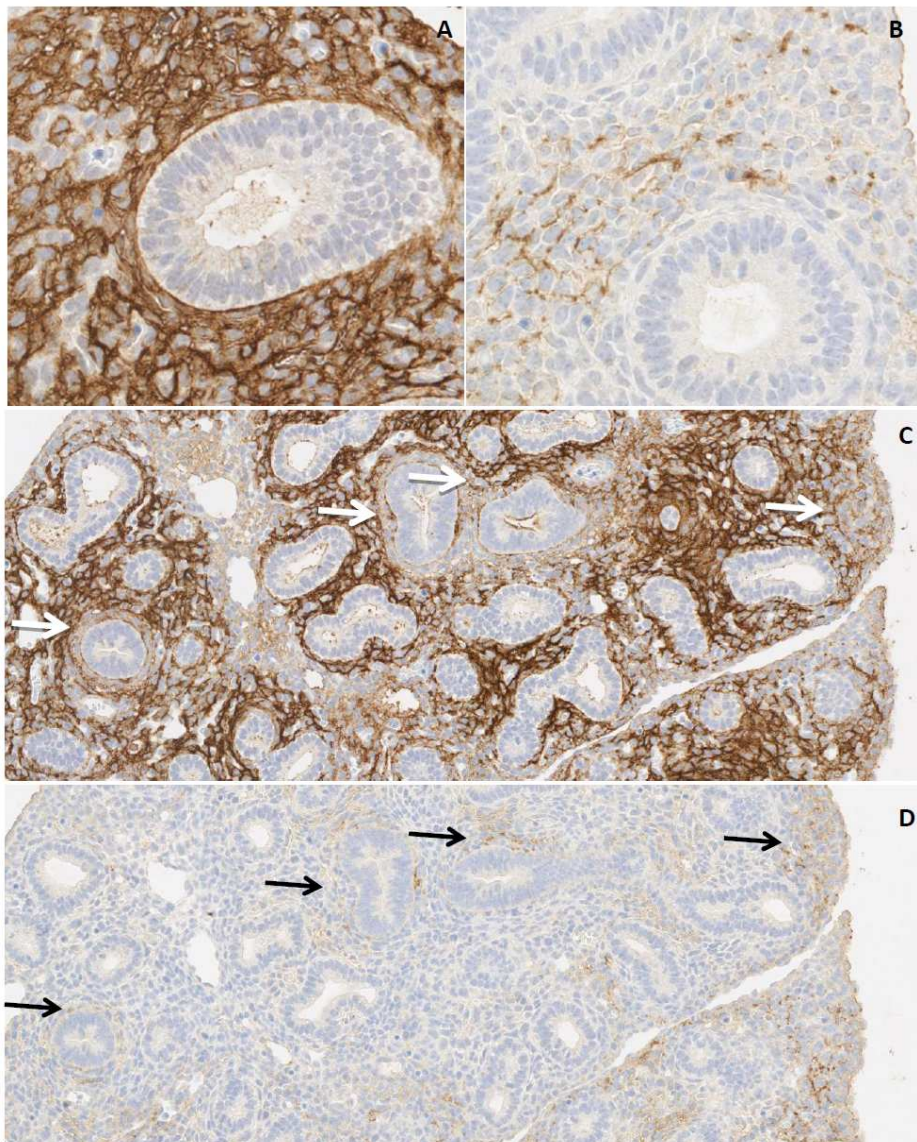


**Figure 19.** There is weaker  $\alpha$ -GAG than  $\beta$ -GAG staining in the whole embryo at E12.5 and E13.5. A and C:  $\alpha$ -GAG immunohistochemistry at (A) E12.5 and (C) E13.5. B and D:  $\beta$ -GAG immunohistochemistry at E12.5 (B) and E13.5 (D). Positive staining for versican  $\alpha$ -GAG and versican  $\beta$ -GAG is brown, with hematoxylin used as a counterstain (blue). Images at 1.25x magnification.

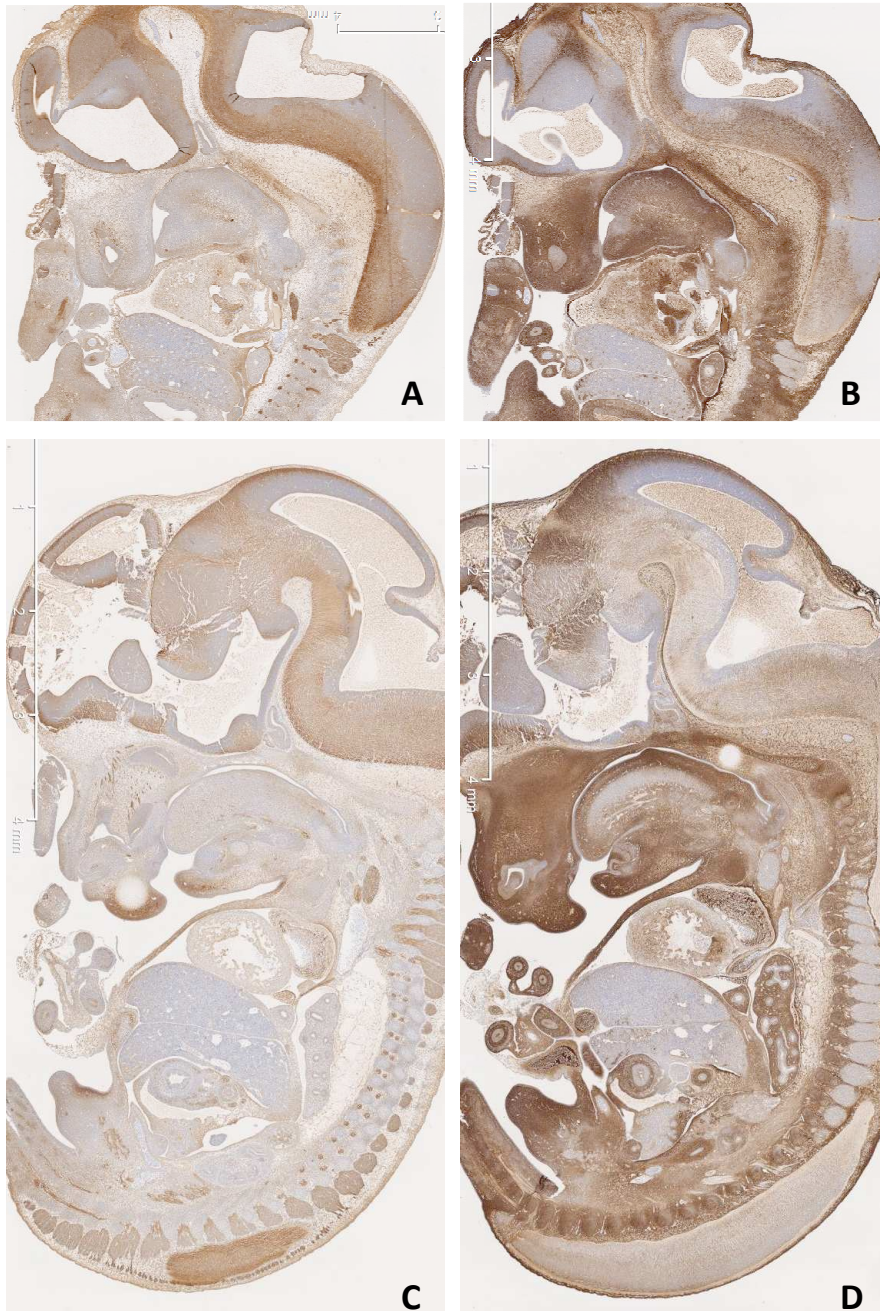
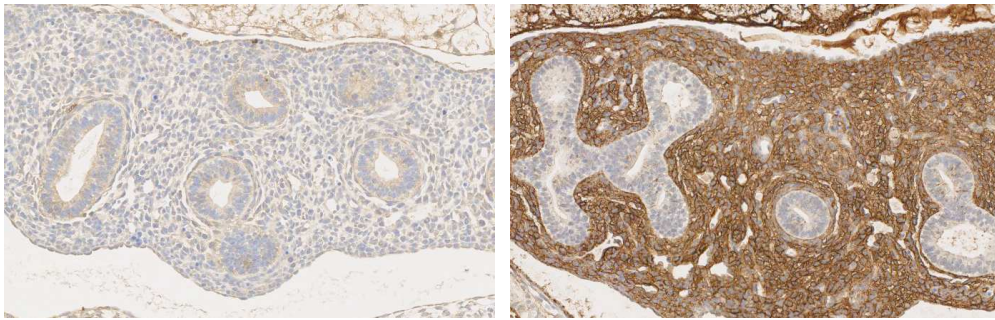
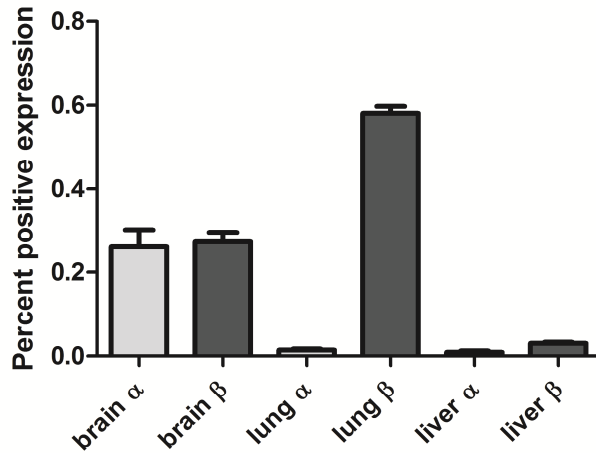


**Figure 20. There is greater  $\alpha$ -GAG immunoreactivity in the brain than in the lung or liver at E13.5.** Top:  $\alpha$ -GAG (left) and  $\beta$ -GAG (right) immunohistochemistry in the lung at E13.5. Bottom: Versican  $\alpha$ -GAG and  $\beta$ -GAG immunoreactivity by quantitative immunohistochemistry by organ at E13.5. Positive staining for versican  $\alpha$ -GAG and versican  $\beta$ -GAG is brown, with hematoxylin used as a counterstain (blue). Images at 5x magnification. Changes in  $\alpha$ -GAG and  $\beta$ -GAG versican quantitative immunohistochemistry were determined by calculating ratio of versican to total tissue area using the visiopharm image analysis module. Values are the mean  $\pm$  SEM.



**Versican  $\alpha$ -GAG and  $\beta$ -GAG immunohistochemistry at E13.5**



## References

1. Zhang, Z.W., et al., *Does the expression of versican isoforms contribute to the pathogenesis of neurodegenerative diseases?* Arch Med Res, 2011. **42**(3): p. 258-60.
2. Shepard, J.B., et al., *Versican expression during synovial joint morphogenesis.* International Journal of Biological Sciences, 2007. **3**(6): p. 380-384.
3. Faggian, J., et al., *Changes in versican and chondroitin sulfate proteoglycans during structural development of the lung.* American Journal of Physiology-Regulatory Integrative and Comparative Physiology, 2007. **293**(2): p. R784-R792.
4. Mjaatvedt, C.H., et al., *The Cspg2 gene, disrupted in the hdf mutant, is required for right cardiac chamber and endocardial cushion formation.* Developmental Biology, 1998. **202**(1): p. 56-66.
5. Hatano, S., et al., *Versican/PG-M is essential for ventricular septal formation subsequent to cardiac atrioventricular cushion development.* Glycobiology, 2012. **22**(9): p. 1268-1277.
6. Wight, T.N., *Versican: a versatile extracellular matrix proteoglycan in cell biology.* Curr Opin Cell Biol, 2002. **14**(5): p. 617-23.
7. Milev, P., et al., *Differential regulation of expression of hyaluronan-binding proteoglycans in developing brain: Aggrecan, versican, neurocan, and brevican.* Biochemical and Biophysical Research Communications, 1998. **247**(2): p. 207-212.
8. Zako, M., et al., *Expression of PG-M(V3), an alternatively spliced form of PG-M without a chondroitin sulfate attachment in region in mouse and human tissues.* J Biol Chem, 1995. **270**(8): p. 3914-8.
9. Zimmermann, D.R. and E. Ruoslahti, *Multiple domains of the large fibroblast proteoglycan, versican.* EMBO J, 1989. **8**(10): p. 2975-81.
10. Horii-Hayashi, N., et al., *Localization of chondroitin sulfate proteoglycan versican in adult brain with special reference to large projection neurons.* Cell Tissue Res, 2008. **334**(2): p. 163-77.
11. Gu, W.L., et al., *Expression and regulation of versican in neural precursor cells and their lineages.* Acta Pharmacol Sin, 2007. **28**(10): p. 1519-30.
12. Sheng, W., et al., *Versican mediates mesenchymal-epithelial transition.* Mol Biol Cell, 2006. **17**(4): p. 2009-20.
13. Sheng, W., et al., *The roles of versican V1 and V2 isoforms in cell proliferation and apoptosis.* Mol Biol Cell, 2005. **16**(3): p. 1330-40.
14. Schmalfeldt, M., et al., *Brain derived versican V2 is a potent inhibitor of axonal growth.* Journal of Cell Science, 2000. **113**(5): p. 807-816.
15. Schmalfeldt, M., et al., *Versican V2 is a major extracellular matrix component of the mature bovine brain.* J Biol Chem, 1998. **273**(25): p. 15758-64.
16. Landolt, R.M., et al., *Versican is selectively expressed in embryonic tissues that act as barriers to neural crest cell migration and axon outgrowth.* Development, 1995. **121**(8): p. 2303-12.
17. Carrino, D.A., et al., *Age-related differences in human skin proteoglycans.* Glycobiology, 2011. **21**(2): p. 257-68.

18. Yamagata, M., T. Shinomura, and K. Kimata, *Tissue variation of two large chondroitin sulfate proteoglycans (PG-M/versican and PG-H/aggrecan) in chick embryos*. *Anat Embryol (Berl)*, 1993. **187**(5): p. 433-44.
19. Matsumoto, K., et al., *Identification and characterization of versican/PG-M aggregates in cartilage*. *Journal of Biological Chemistry*, 2006. **281**(26): p. 18257-18263.
20. Wu, Y.J., et al., *The interaction of versican with its binding partners*. *Cell Res*, 2005. **15**(7): p. 483-94.
21. Casini, P., et al., *Identification and gene expression of versican during early development of Xenopus*. *International Journal of Developmental Biology*, 2008. **52**(7): p. 993-998.
22. Bensadoun, E.S., et al., *Proteoglycans in granulomatous lung diseases*. *Eur Respir J*, 1997. **10**(12): p. 2731-7.
23. Gill, S., T.N. Wight, and C.W. Frevert, *Proteoglycans: key regulators of pulmonary inflammation and the innate immune response to lung infection*. *Anat Rec (Hoboken)*, 2010. **293**(6): p. 968-81.
24. Deepa, S.S., et al., *Composition of perineuronal net extracellular matrix in rat brain: a different disaccharide composition for the net-associated proteoglycans*. *J Biol Chem*, 2006. **281**(26): p. 17789-800.
25. Asher, R.A., et al., *Versican is upregulated in CNS injury and is a product of oligodendrocyte lineage cells*. *J Neurosci*, 2002. **22**(6): p. 2225-36.
26. Sobel, R.A. and A.S. Ahmed, *White matter extracellular matrix chondroitin sulfate/dermatan sulfate proteoglycans in multiple sclerosis*. *J Neuropathol Exp Neurol*, 2001. **60**(12): p. 1198-207.
27. Fawcett, J.W. and R.A. Asher, *The glial scar and central nervous system repair*. *Brain Res Bull*, 1999. **49**(6): p. 377-91.
28. Bensadoun, E.S., et al., *Proteoglycan deposition in pulmonary fibrosis*. *Am J Respir Crit Care Med*, 1996. **154**(6 Pt 1): p. 1819-28.
29. Merrilees, M.J., et al., *Changes in elastin, elastin binding protein and versican in alveoli in chronic obstructive pulmonary disease*. *Respir Res*, 2008. **9**: p. 41.
30. Lowry, M.H., et al., *Lung lining fluid glutathione attenuates IL-13-induced asthma*. *Am J Respir Cell Mol Biol*, 2008. **38**(5): p. 509-16.
31. Naso, M.F., et al., *Expression pattern and mapping of the murine versican gene (Cspg2) to chromosome 13*. *Genomics*, 1995. **29**(1): p. 297-300.
32. Wu, Y., et al., *Versican V1 isoform induces neuronal differentiation and promotes neurite outgrowth*. *Mol Biol Cell*, 2004. **15**(5): p. 2093-104.
33. Perissinotto, D., et al., *Avian neural crest cell migration is diversely regulated by the two major hyaluronan-binding proteoglycans PG-M/versican and aggrecan*. *Development*, 2000. **127**(13): p. 2823-2842.
34. Dutt, S., et al., *Versican V0 and V1 guide migratory neural crest cells*. *Journal of Biological Chemistry*, 2006. **281**(17): p. 12123-12131.
35. Popp, S., et al., *Localization of aggrecan and versican in the developing rat central nervous system*. *Developmental Dynamics*, 2003. **227**(1): p. 143-149.
36. Oohashi, T., et al., *Brall1, a brain-specific link protein, colocalizing with the versican V2 isoform at the nodes of Ranvier in developing and adult mouse central nervous systems*. *Mol Cell Neurosci*, 2002. **19**(1): p. 43-57.

37. Henderson, D.J. and A.J. Copp, *Versican expression is associated with chamber specification, septation, and valvulogenesis in the developing mouse heart*. *Circulation Research*, 1998. **83**(5): p. 523-532.
38. Adhikari, N., et al., *Changes in Expression of Proteoglycan Core Proteins and Heparan Sulfate Enzymes in the Developing and Adult Murine Aorta*. *Journal of Cardiovascular Translational Research*, 2011. **4**(3): p. 313-320.
39. Rutter, M., et al., *Gli2 influences proliferation in the developing lung through regulation of cyclin expression*. *Am J Respir Cell Mol Biol*, 2010. **42**(5): p. 615-25.
40. McCulloch, D.R., et al., *Adamts5, the gene encoding a proteoglycan-degrading metalloprotease, is expressed by specific cell lineages during mouse embryonic development and in adult tissues*. *Gene Expression Patterns*, 2009. **9**(5): p. 314-323.
41. Snow, H.E., et al., *Versican expression during skeletal/joint morphogenesis and patterning of muscle and nerve in the embryonic mouse limb*. *Anatomical Record Part a- Discoveries in Molecular Cellular and Evolutionary Biology*, 2005. **282A**(2): p. 95-105.
42. Smith, S.M., et al., *Topographical variation in the distributions of versican, aggrecan and perlecan in the foetal human spine reflects their diverse functional roles in spinal development*. *Histochem Cell Biol*, 2009. **132**(5): p. 491-503.
43. Stanton, H., et al., *Proteoglycan degradation by the ADAMTS family of proteinases*. *Biochim Biophys Acta*, 2011. **1812**(12): p. 1616-29.
44. Kenagy, R.D., A.H. Plaas, and T.N. Wight, *Versican degradation and vascular disease*. *Trends Cardiovasc Med*, 2006. **16**(6): p. 209-15.
45. Porter, S., et al., *The ADAMTS metalloproteinases*. *Biochem J*, 2005. **386**(Pt 1): p. 15-27.
46. Capehart, A.A., *Proteolytic Cleavage of Versican During Limb Joint Development*. *Anatomical Record-Advances in Integrative Anatomy and Evolutionary Biology*, 2010. **293**(2): p. 208-214.
47. Russell, D.L., et al., *Processing and localization of ADAMTS-1 and proteolytic cleavage of versican during cumulus matrix expansion and ovulation*. *J Biol Chem*, 2003. **278**(43): p. 42330-9.
48. Sandy, J.D., et al., *Versican VI proteolysis in human aorta in vivo occurs at the Glu441-Ala442 bond, a site that is cleaved by recombinant ADAMTS-1 and ADAMTS-4*. *J Biol Chem*, 2001. **276**(16): p. 13372-8.
49. Longpre, J.M., et al., *Characterization of proADAMTS5 processing by proprotein convertases*. *International Journal of Biochemistry & Cell Biology*, 2009. **41**(5): p. 1116-1126.
50. Kern, C.B., et al., *Proteolytic cleavage of versican during cardiac cushion morphogenesis*. *Developmental Dynamics*, 2006. **235**(8): p. 2238-2247.
51. Kern, C.B., et al., *Versican proteolysis mediates myocardial regression during outflow tract development (vol 236, pg 671, 2007)*. *Developmental Dynamics*, 2007. **236**(4): p. 1157-1157.
52. Gunther, W., et al., *Distribution patterns of the anti-angiogenic protein ADAMTS-1 during rat development*. *Acta Histochem*, 2005. **107**(2): p. 121-31.
53. Thai, S.N.M. and M.L. Iruela-Arispe, *Expression of ADAMTS1 during murine development*. *Mechanisms of Development*, 2002. **115**(1-2): p. 181-185.

54. Dupuis, L.E., et al., *Altered versican cleavage in ADAMTS5 deficient mice; A novel etiology of myxomatous valve disease*. *Developmental Biology*, 2011. **357**(1): p. 152-164.
55. Shindo, T., et al., *ADAMTS-1: a metalloproteinase-disintegrin essential for normal growth, fertility, and organ morphology and function*. *J Clin Invest*, 2000. **105**(10): p. 1345-52.
56. Little, C.B., et al., *ADAMTS-1-knockout mice do not exhibit abnormalities in aggrecan turnover in vitro or in vivo*. *Arthritis Rheum*, 2005. **52**(5): p. 1461-72.
57. McCulloch, D.R., et al., *ADAMTS metalloproteases generate active versican fragments that regulate interdigital web regression*. *Dev Cell*, 2009. **17**(5): p. 687-98.
58. Enomoto, H., et al., *Cooperation of two ADAMTS metalloproteases in closure of the mouse palate identifies a requirement for versican proteolysis in regulating palatal mesenchyme proliferation*. *Development*, 2010. **137**(23): p. 4029-38.
59. Kaufman, M., *The Atlas of Mouse Development*. Second Printing of First Edition 1995, San Diego, CA: Academic Press, Inc.
60. Chang, M.Y., et al., *A rapid increase in macrophage-derived versican and hyaluronan in infectious lung disease*. *Matrix Biol*, 2014.
61. Livak, K.J. and T.D. Schmittgen, *Analysis of relative gene expression data using real-time quantitative PCR and the 2<sup>-Delta Delta C(T)</sup> Method*. *Methods*, 2001. **25**(4): p. 402-8.
62. Crawford, L.W., J.F. Foley, and S.A. Elmore, *Histology atlas of the developing mouse hepatobiliary system with emphasis on embryonic days 9.5-18.5*. *Toxicol Pathol*, 2010. **38**(6): p. 872-906.
63. Savolainen, S.M., J.F. Foley, and S.A. Elmore, *Histology atlas of the developing mouse heart with emphasis on E11.5 to E18.5*. *Toxicol Pathol*, 2009. **37**(4): p. 395-414.
64. Jungers, K.A., et al., *Adamts9 is widely expressed during mouse embryo development*. *Gene Expr Patterns*, 2005. **5**(5): p. 609-17.
65. Shannon, J.M., et al., *Chondroitin sulfate proteoglycans are required for lung growth and morphogenesis in vitro*. *Am J Physiol Lung Cell Mol Physiol*, 2003. **285**(6): p. L1323-36.
66. Nandadasa, S., et al., *The multiple, complex roles of versican and its proteolytic turnover by ADAMTS proteases during embryogenesis*. *Matrix Biol*, 2014. Article in press.